https://doi.org/10.5194/egusphere-2026-1389
Preprint. Discussion started: 25 March 2026

The Northernmost Mountain Belt on Earth: Birth and Death of the Eurekan Orogen in North Greenland

Katrin Meier[1], Paul O'Sullivan[2], David Chew[3], Karsten Piepjohn[4], Solveig Estrada[4], Nikola Koglin[5], Patrick Monien[1], Frank Lisker[1], Cornelia Spiegel[1]

[1]Department of Geosciences, University of Bremen, Bremen, Germany
[2]GeoSep Services, Moscow, ID, USA
[3]Department of Geology, Trinity College Dublin, Dublin, Ireland
[4]retired from Federal Institute for Geosciences and Natural Resources (BGR), Hannover, Germany
[5]Federal Institute for Geosciences and Natural Resources (BGR), Hannover, Germany

Correspondence to: Katrin Meier (k.meier@uni-bremen.de)

Abstract. The >1000 km long Eurekan Belt is the northernmost mountain belt on Earth and formed as an intraplate orogen in response to Cenozoic plate reorganization of the North Atlantic–Arctic region. Eurekan deformation is well documented on Ellesmere Island, North Greenland and Svalbard. In North Greenland, the general orientation of the Eurekan Belt changes. The kinematic and temporal relationships between the differently trending fault systems of North Greenland remain poorly constrained. This study aims to explore the relationship between the major fault systems of North Greenland by providing a temporal framework for their kinematics. We present new low-temperature thermochronological data, including the first apatite (U-Th)/He ages from North Greenland, complemented by apatite fission track analyses and apatite U–Pb dating of mafic dykes. Thermal history models indicate a short-lived heating period during the latest Cretaceous (~70–65 Ma), with temperatures exceeding 120 °C, likely associated with a Late Cretaceous basin along the margin of North Greenland. The models imply repeated reactivation of the Kap Cannon Thrust Zone, the Harder Fjord Fault Zone and the Trolle Land Fault System during the Palaeocene, early and mid-Eocene, and Oligocene. The differently oriented fault systems constitute a coherent system, interpreted as part of the De Geer Fracture Zone, that was repeatedly reactivated under changing stress fields. The exhumation episodes of North Greenland were synchronous with those of adjacent regions of the Eurekan Belt. Oligocene exhumation of North Greenland can be linked to tectonic reorganization of the northern North Atlantic and the opening of the Proto-Fram Strait, which likely developed along pre-existing structural weaknesses. Together, these findings highlight the role of structural inheritance, thermal weakening, and fault reactivation in intraplate orogeny and provide temporal constraints on the tectonic and topographic evolution of the Arctic relevant to paleogeographic and high-latitude environmental reconstructions.

https://doi.org/10.5194/egusphere-2026-1389
Preprint. Discussion started: 25 March 2026

1 Introduction

The Eurekan Belt is an intraplate orogen which stretches for several thousand kilometres along the margin of the Arctic Ocean (Fig. 1a). Deformation associated with this mountain belt is mainly documented on Ellesmere Island, Greenland and Svalbard (Piepjohn et al., 2016 and references therein) but may have also affected the East Siberian Shelf and the Arctic Ocean (Døssing et al., 2014; Gaina et al., 2015; O'Regan et al., 2008). The Cenozoic formation of the Eurekan Belt is directly linked to plate reorganisation of the northern hemisphere and the opening of the northern North Atlantic Ocean. It accommodated shortening within the then-continuous continental landmasses of Laurentia, Greenland, and Baltica. Mechanisms behind intraplate orogeny are still not fully understood. According to classical plate tectonic theory, compressive stress is focussed along the plate margins, whereas plate interiors are considered as rigid and hard to deform (e.g., McKenzie and Parker, 1967; Morgan, 1968). Other examples for intraplate orogeny involve the recent Tien Shan and Altai Mountains in Central Asia or the ancient Alice Spring and Petermann Orogen in Australia (Raimondo et al., 2014 and references therein).

Formation of the Eurekan Belt was strongly episodic (Fig. 1b). First movements, here referred to as pre-Eurekan stage, occurred during the Late Cretaceous to Palaeocene, when rifting and spreading of the Labrador Sea/Baffin Bay initiated (Oakey and Chalmers, 2012; Roest and Srivastava, 1989). The onset of spreading of the Norwegian-Greenland Sea resulted in Greenland acting as an independent microplate during the Eocene. It moved northward and rotated anticlockwise, causing the Eurekan Orogeny (de Paor et al., 1989; Srivastava, 1985; Talwani and Eldholm, 1977; Tessensohn and Piepjohn, 2000). The first stage of the Eurekan (Eurekan I) was associated with NE-SW contraction along the present west coast of Spitsbergen, contemporaneously with sinistral strike-slip movements along the NE-SW striking Wegener Fault between Northwest Greenland and Ellesmere Island (Fig. 1b). The second stage of the Eurekan (Eurekan II) involved NW-SE dextral strike-slip motions along the De Geer Fracture Zone between eastern North Greenland and Svalbard on the one side, and SE contraction across Nares Strait on Ellesmere Island on the other side (Piepjohn et al., 2016).

At about the Eocene-Oligocene transition, spreading of the Labrador Sea/Baffin Bay terminated, whereas spreading of the Norwegian-Greenland Sea was ongoing, so that Greenland ceased to move independently and became part of the North American plate (Kristoffersen and Talwani, 1977; Talwani and Eldholm, 1977). Movements along the De Geer Fracture Zone continued but changed from transpressional to transtensional. We refer to the deformation associated with these transtensional movements as the post-Eurekan stage (Fig. 1b). Exhumation associated with the different stages of Eurekan deformation was dated by low-temperature thermochronology on northern Ellesmere Island (Vamvaka et al., 2019). These data revealed rapid exhumation between ~66-60 Ma for the pre-Eurekan, between 55-48 Ma and 44-38 Ma for Eurekan I and II, and between ~34–26 Ma for the post-Eurekan, with intermittent periods of slow exhumation (Fig. 1c). The different stages were correlated with changes in spreading rates and directions of the Norwegian-Greenland Sea (Vamvaka et al., 2019). Finally, during the Oligocene, seafloor spreading of the Norwegian-Greenland Sea propagated northwards and eventually the spreading ridges of the Norwegian-Greenland Sea and the Eurasian Basin of the Arctic Ocean merged. This led to the Miocene opening of the Fram Strait (Engen et al., 2008; Jokat et al., 2016) and the dissection of the Eurekan Belt (Fig.1a).

https://doi.org/10.5194/egusphere-2026-1389
Preprint. Discussion started: 25 March 2026

North Greenland includes the central segment of the Eurekan Belt, and it is also the place where the Eurekan Belt changes its dominant direction of strike: In northern North Greenland, deformation is focussed along two major, ~E-W to SW-NE-striking compressional fault zones, the Kap Cannon Thrust Zone and the Harder Fjord Fault Zone (Fig. 1a; von Gosen and Piepjohn, 1999; Lyberis and Manby, 2001; Piepjohn and von Gosen, 2001). Eastern North Greenland, by contrast, is dominated by the NW-SE-striking compressional or transpressional Trolle Land Fault System (Fig. 1a; von Gosen and Piepjohn, 2003; Lyberis and Manby, 2001; Pedersen and Håkansson, 2001). Cross-cutting relationships between these two regional structural trends are rare and difficult to interpret, and hence, their kinematic and temporal relationships remain unclear (Paech and Estrada, 2019; Soper and Higgins, 1991). Håkansson and Pedersen (1982) assume simultaneous activity of all fault systems, and Pedersen and Håkansson (2001) suggest that the strike-slip movements were transmitted to the north-west via the Harder Fjord Fault Zone. In contrast, Lyberis and Manby (2001) interpret from field observations that the Harder Fjord Fault Zone intersects the Trolle Land Fault Zone. Von Gosen and Piepjohn (2003) also point out this possibility but also consider simultaneous activity to be possible. This makes it difficult to relate the Eurekan structures of North Greenland to those of Ellesmere Island and Svalbard, and to integrate the activity of the fault systems into a larger geodynamic context. In addition, the age of deformation along the different structures is still debated. Models include deformation during the Late Cretaceous to Palaeogene (Lyberis and Manby, 2001; Pedersen and Håkansson, 2001; Zinck-Jørgensen, 1994b), during the Palaeocene to Eocene (Soper et al., 1982; Svennevig et al., 2016) or only during the Eocene (von Gosen and Piepjohn, 2003; Piepjohn et al., 2016).

Our study aims to explore the relationship between the major fault systems of North Greenland, namely the Kap Cannon Thrust Zone, the Harder Fjord Fault Zone and the Trolle Land Fault System, by providing a time framework for their kinematics. This allows to make inferences on the kinematic, spatial and temporal relationships between the different structural segments of the Eurekan Belt in North Greenland. To address this goal, we use low-temperature thermochronological dating methods and provide the first apatite (U-Th)/He data from North Greenland, along with new apatite fission track data. Moreover, we apply apatite U-Pb dating to previously undated mafic dykes. Our results contribute to a better understanding of the Eurekan deformation and its preceding tectonic processes and also contribute to the general knowledge of intraplate orogenies.

A further aspect of this study focusses on the climatic relevance of the Eurekan orogen as the northernmost mountain belt of the planet, formed at a time – the Eocene - when a permanent continental ice sheet established in Antarctica that profoundly changed Earth´s climate (e.g. Francis et al., 2008). Some evidence suggests formation of continental ice also in the Arctic (Eldrett et al., 2007; Schouten et al., 2008; Spielhagen and Tripati, 2009; Stickley et al., 2009; Tripati et al., 2008), but detailed conditions for Arctic ice formation during the relatively warm climate of the Eocene are still poorly understood (Fig. 1c). Hence, studying processes that led to high-latitude mountain building and topography formation may improve our understanding of Arctic climate evolution (e.g. Langebroek et al., 2017).

https://doi.org/10.5194/egusphere-2026-1389
Preprint. Discussion started: 25 March 2026

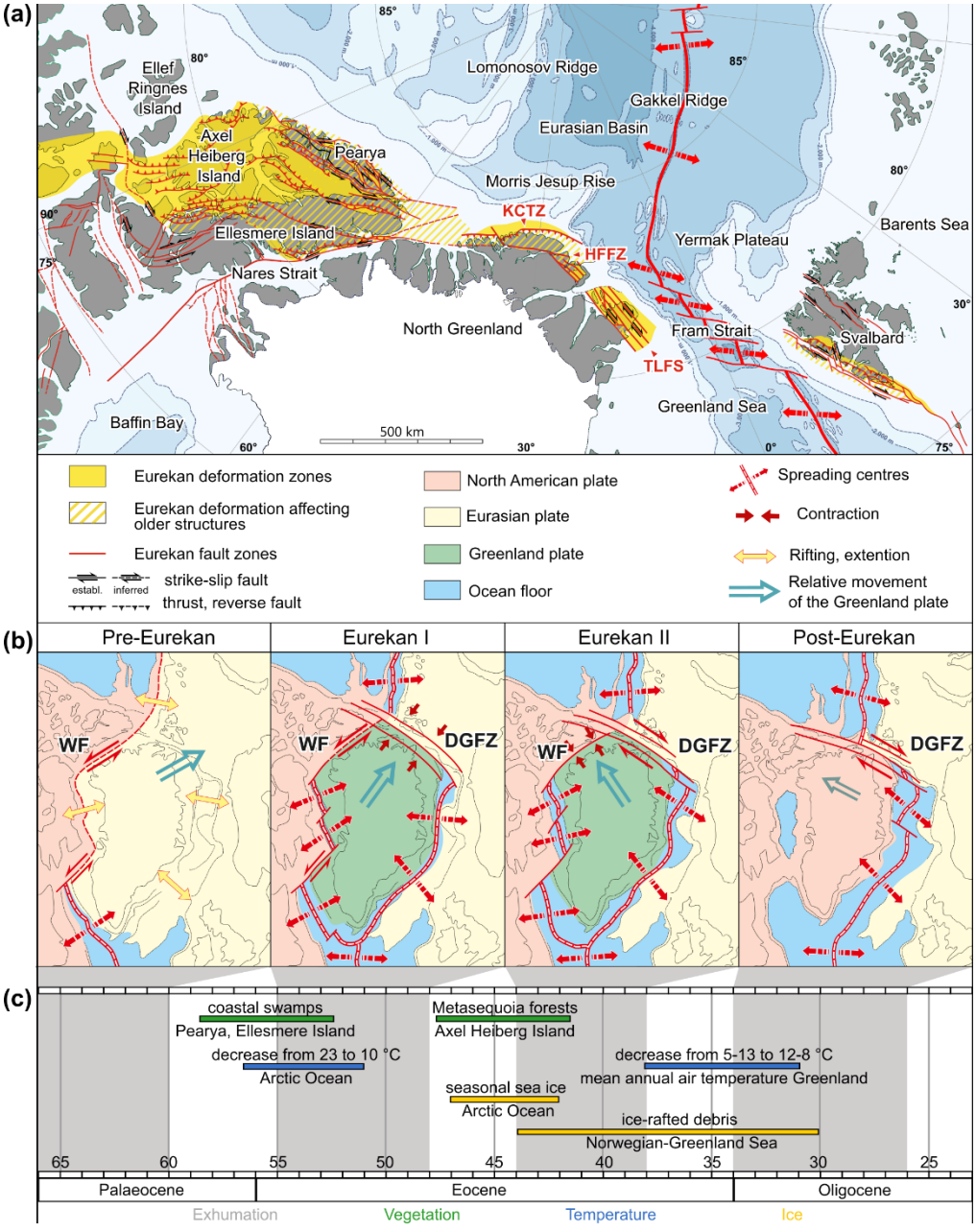

Figure 1: Overview and conceptual model illustrating the formation, evolution, and climatic context of the Eurekan Belt. (a) Extent of the Eurekan Belt across Svalbard, North Greenland, and the Canadian Arctic Archipelago, showing deformation and the major fault systems (KCTZ – Kap Cannon Thrust Zone, HFFZ – Harder Fjord Fault Zone, TLFS – Trolle Land Fault System) modified from Piepjohn et al. (2015). (b) Conceptual model showing the tectonic evolution during the pre-Eurekan, Eurekan I–II , and post-Eurekan stages. (WF – Wegener Fault, DGFZ – De Geer Fracture Zone) modified from Piepjohn et al. (2016). (c) Temporal framework showing the timing of Eurekan exhumation phases highlighted in grey (pre-Eurekan (~66–60 Ma), EurekanI–II (~55–38 Ma), post-Eurekan (~34–26 Ma) after Vamvaka et al. (2019) and indicators of climatic change, including vegetation (Jahren and Sternberg, 2008), temperature (Schouten et al., 2008), and sea and continental ice development (Stickley et al., 2009; Tripati et al., 2008).

https://doi.org/10.5194/egusphere-2026-1389
Preprint. Discussion started: 25 March 2026

2 Geological setting – structures and sedimentary sequences of North Greenland

The geology of North Greenland is dominated by the Cambrian to Silurian sediments of the Franklinian Basin, which were deposited on Precambrian basement along the passive continental margin of Laurentia (Fig. 2). In northern North Greenland, the Franklinian deposits were deformed by the late Devonian to early Carboniferous Ellesmerian Orogeny, forming the approximately east-west striking North Greenland Fold Belt (e.g., Higgins, 1986). Likewise, the Eurekan structures of northern North Greenland are mostly east-west-oriented. The eastern margin of Greenland, by contrast, is dominated by the Silurian north-south-striking Caledonian orogenic belt. At the site where the Ellesmerian and the Caledonian belts intersect along the eastern corner of North Greenland, the northwest-southeast striking Wandel Hav Mobile Belt has formed (Håkansson and Pedersen, 2015), which represents the eastern North Greenland segment of the Eurekan Belt (von Gosen and Piepjohn, 2003). Subsequent to the Ellesmerian and Caledonian orogenies, the Wandel Sea Basin formed, whose Carboniferous to Cretaceous deposits are preserved as isolated patches across North Greenland (Fig. 2, Fig.4, Fig.5, Fig. 6, Fig.7; Håkansson and Pedersen, 2015; Håkansson and Stemmerik, 1989).

2.2 Northern North Greenland

In northern North Greenland, the Wandel Sea Basin deposits consist of Late Cretaceous non-marine shales (Batten et al., 1981; Brown and Parsons, 1981) conformably covered by the Late Cretaceous to Palaeocene Kap Washington Group (Fig. 2A; Fig. 5). The up to 5 km thick Kap Washington Group comprises bimodal volcanic flows and pyroclastics, interbedded with layers of sandstone- and shales (Batten, 1982; Brown et al., 1987; Brown and Parsons, 1981; Estrada et al., 2001). The volcanic rocks yield ages between 71 and 61 Ma (Tegner et al., 2011; Thórarinsson et al., 2011a), with younger ages on Lockwood Island, as compared to those at Kap Kane towards the East. The shales interbedded with the volcanogenic rocks contain pollen, which suggest a Maastrichtian depositional age (Batten, 1982). They show a high thermal maturity with vitrinite reflectance values between 2.6 and 5.4 % (Fig. 2-1; Paech and Estrada, 2019). The Cretaceous and older deposits of the Franklinian Basin were intruded by Late Cretaceous dykes (Fig. 2). These north-south, northwest-southeast and east-west- trend dykes yield Ar-Ar and U/Pb ages between 85 Ma and 80 Ma, with minimal age differences between the different spatial orientations of the dykes (Buchan and Ernst, 2006, 2018; Kontak et al., 2001; Thórarinsson et al., 2015).

The main Eurekan structural elements of northern North Greenland are the east-west trending Harder Fjord Fault Zone and the southwest-northeast trending Kap Cannon Thrust Zone (Fig. 2, Fig. 5, Fig. 6). Both comprise a set of individual fault structures interpreted as dominated by orthogonal north-south compression (Piepjohn et al., 2015).

Our study of the Kap Cannon Thrust Zone focuses on the area of Lockwood Island (Fig. 2A, Fig. 5a). Here, we distinguish three different, fault-delimited blocks, following the structural interpretation of von Gosen and Piepjohn (1999). The southern block comprises metamorphosed Palaeozoic sequences. It was juxtaposed with the central block along the Kap Cannon Thrust. Within the southern block, mylonites are developed, associated with N-S compressional stress (von Gosen and Piepjohn, 1999; Lyberis and Manby, 2001). These mylonites also occur along the northeast-continuation of the Kap Cannon Thrust, i.e., in the

https://doi.org/10.5194/egusphere-2026-1389
Preprint. Discussion started: 25 March 2026

Kap Kane, Kap Washington, and Kap Cannon areas (Fig. 5a). Mylonitization deformed, amongst other units, Late Cretaceous dykes within the Palaeozoic sequences of the southern block, suggesting a post Late Cretaceous deformation age (cf. Lyberis and Manby, 2001; Soper et al., 1982). The central block of Lockwood Island comprises Cretaceous volcanogenic deposits of the Kap Washington Group. Unlike the southern block, they are mostly affected by brittle deformation associated with NNW-directed thrusting, suggesting later deformation at a shallower crustal level (von Gosen and Piepjohn, 1999). To the north, the central block is again juxtaposed with Palaeozoic sequences. These Palaeozoic sequences form the northern block, and are separated from the central block by an undefined fault structure, which we name Kap Christiansen Fault. The Kap Christiansen Fault cuts off an earlier thrust within the northern block called Kap Christiansen Thrust (von Gosen and Piepjohn, 1999, their Fig. 6).

South of the Kap Cannon Thrust Zone, the Harder Fjord Fault Zone extends in an east-west direction over a length of about 250 km from the coast of the Wandel Sea in the east, to Nansen Land in the west (Fig. 2, Fig. 6a; Soper and Higgins, 1987). To the east, it forms a graben-like structure that tapers westward (Soper and Higgins, 1991). In the central part of the fault zone, fault-bound sediments of Wandel Hav Basin and deformed ”greenstones of unknown age” (Higgins et al., 1981) are preserved (Fig. 2B-2). Based on their chemical composition, the “greenstones” are interpreted as tectonically fragmented equivalents to the late Cretaceous dykes (Estrada, 2000). So far, they have not been dated by radiometric methods. East of the “greenstones”, at the Santon Glacier, Late Cretaceous, presumably Santonian, sediments are exposed (Fig. 2B-3; Birkelund and Håkansson, 1983; Piepjohn and von Gosen, 2001). These sandstone-dominated, shallow marine deposits are approximately 500 m thick and rest on a basal erosion surface (Piepjohn and von Gosen, 2001). Their relationship to the sediments of the Kap Washington Group exposed further north is unclear. The sedimentary rocks show vitrinite reflectance values between 2.7 and 3.6% (Paech and Estrada, 2019). They are nearly vertically dipping to slightly overturned and are bounded by reverse faults to the north and south.

Along the eastern part of the Harder Fjord Fault Zone, in the Depot Bugt area (Fig. 2C-4), conglomerates and poorly sorted sandstones and siltstones are exposed. They are about 500 m thick, presumably of fluvial origin (Håkansson and Pedersen, 2015), with vitrinite reflectance values of 1.9 to 2.2 % (Paech and Estrada, 2019), and contain plant fossils (Birkelund and Håkansson, 1983; Piepjohn and von Gosen, 2001). However, age diagnostic fossils are missing, but, based on correlations with the Herlufsholm Strand Formation exposed further south, a Late Cretaceous depositional age is assumed (Birkelund and Håkansson, 1983). Again, the relationship to the other Late Cretaceous deposits exposed in North Greenland is unclear. The Late Cretaceous deposits of the Depot Bugt area are overlain by dark, flat lying carbonaceous shales with a shattered and in places rusty appearance, probably with an unconformity in between the units (Croxton et al., 1980; Paech and Estrada, 2019). The shales are non-marine, have a low coal rank (Håkansson et al., 1981), and contain wood and coal fragments as well as pollen, which indicate a Palaeogene age (Croxton et al., 1980).

https://doi.org/10.5194/egusphere-2026-1389
Preprint. Discussion started: 25 March 2026

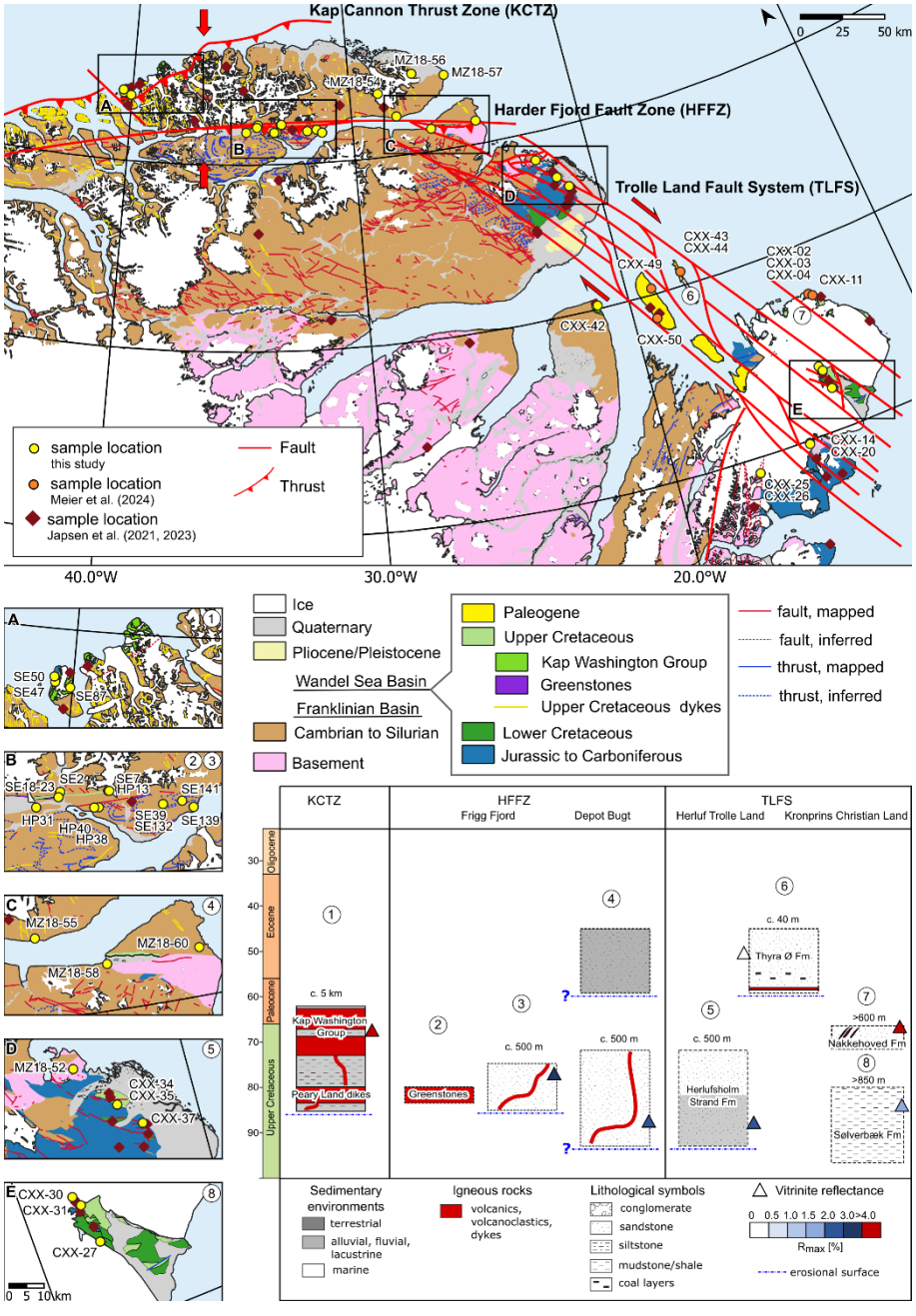

Figure 2: Overview of the Kap Cannon Thrust Zone (KCTZ), Harder Fjord Fault Zone (HFFZ) and Trolle Land Fault System (TLFS) in North Greenland (modified from Kokfelt et al., 2023 and Piepjohn et al. 2016), showing their relationship to preserved Late Cretaceous to Paleogene deposits of the Wandel Sea basin and sample locations of this study and previous work (Japsen et al., 2021, 2023; Meier et al., 2024). Insets highlight deposit occurrence of A) Lockwood Island to Kap Washington, B) Frigg Fjord, C) Depot Bugt D) Herluf Trolle Land and E) Kilen. The stratigraphic chart summarizes the age, maturity and lithology of the deposits for the respective localities (1-8; (Batten, 1982; Brown and Parsons, 1981; Croxton et al., 1980; Estrada, 2000; Guarnieri et al., 2025a, b; Håkansson et al., 1994; Hovikoski et al., 2018; Lyck and Stemmerik, 2000; Paech and Estrada, 2019; Piasecki et al., 2018; Svennevig et al., 2018; Thórarinsson et al., 2011a, 2015).

https://doi.org/10.5194/egusphere-2026-1389
Preprint. Discussion started: 25 March 2026

The deformation style along the Harder Fjord Fault Zone is not fully understood. The long, linear outline of the fault zone would actually suggest strike-slip movements (Piepjohn et al., 2015; Soper and Higgins, 1991), and indeed, along the western part of the fault zone, a possible Cretaceous or Cenozoic dextral displacement of ca. 20 km was inferred (Soper and Higgins, 1987). However, Piepjohn and von Gosen (2001) mainly observed structures indicating north-south compression during the Eurekan whereas kinematic indicators of strike-slip movement are restricted to the easternmost Harder Fjord Fault Zone. Solfatara deposits in the Depot Bugt and earthquake activity suggest that the Harder Fjord Fault Zone may still be active today, associated with transtensional movements (Chung, 2002; Croxton et al., 1980; Dawes and Peel, 1981; Gregersen, 1982). Besides the approximately east-west striking faults, the Harder Fjord Fault Zone is internally dissected by numerous smaller individual faults, whose characteristics and ages are unknown (Fig. 6a). Strike directions are highly variable and include southwest-northeast as well as southeast-northwest trends.

2.3 Eastern North Greenland

The eastern part of North Greenland is characterized by the Trolle Land Fault System, a northwest-southeast-trending fault system of slightly fan-shaped to almost parallel faults, which is interpreted to be part of the larger De Geer Fracture Zone (Fig. 2, Fig. 7a; von Gosen and Piepjohn, 2003; Håkansson and Pedersen, 2001; Meier et al., 2024; Svennevig et al., 2016). In Herluf Trolle Land, the youngest deposits affected by the fault activity are those of the Herlufsholm Strand Formation (Fig. 2D-5). The stratigraphic age of this formation was until recently poorly constrained. It contains remnants of wood and plants, which suggest a late Cretaceous to early Paleogene deposition age (Winther et al., 1950). The occurrence of inoceramid bivalves implies a Turonian to Coniacian age (Håkansson, 1994), while U-Pb ages of detrital zircons suggest a Campanian or younger depositional age (Guarnieri et al., 2025b). The formation comprises sandstone-shale alternations of about 500 m thickness that rest unconformably on Carboniferous to Permian strata. The deposits are partly of fluvial origin and partly marine, with the latter occurring only within a thrust-bound fault block in the southeast (Zinck-Jørgensen, 1994a). The thermal maturity of the deposits differs, with vitrinite reflectance values of 2.5 % - 3.1 % in the east and 1.1 % - 1.7 % in the west (Paech and Estrada, 2019). In Kronprins Christian Land, the youngest deposits affected by the fault activity are those of the marine Sølverbæk Formation in the Kilen Fjelde and Gåseslette area (Fig. 2E-8). Its stratigraphic age was constrained to late Cenomanian to possibly earliest Campanian based on inoceramids, dinoflagellate cysts and ammonites (Hovikoski et al., 2018). The 600-850 m thick formation comprises mudstone, layers of sandstone and sideritic conglomerates (Svennevig et al., 2018). The thermal maturity of the deposits is indicated by vitrinite reflectance values 1.6 % - 2.2 % (Håkansson et al., 1994; Paech and Estrada, 2019). The Nakkehoved Fm on the northeastern coast of Kronprins Christian Land (Fig. 2-7) is possibly even younger, Maastrichtian to Danian (Guarnieri et al., 2025a, b; Meier et al., 2024; Svennevig et al., 2018), and with vitrinite values up to 7 - 10 % (Håkansson et al., 1994). It appears only weakly deformed (Birkelund and Håkansson, 1983).

The Trolle Land Fault System is characterized by dextral strike-slip movements (Fig. 2), causing folding of the Herlufsholm Strand Formation and Sølverbæk Formation in east-west direction, and, close to fault zones, shearing and reverse faulting in an overall north-south to northwest-southeast compressional stress field (von Gosen and Piepjohn, 2003; Lyberis and Manby,

https://doi.org/10.5194/egusphere-2026-1389
Preprint. Discussion started: 25 March 2026

2001; Pedersen and Håkansson, 2001; Svennevig et al., 2016). The timing of the deformation is still debated. Håkansson and Pedersen (1982, 2015) suggest that the deformation along the Trolle Land Fault System, as well as that of northern North Greenland, occurred at the Cretaceous-Palaeogene boundary during a short-lived "Kronprins Christian Land Orogeny", which they assume to be independent from the Eurekan Orogeny. This interpretation is based on the observation that the youngest strata affected by the deformation are of Late Cretaceous age, whereas Palaeogene deposits (Fig. 2-6) were not deformed. By contrast, von Gosen and Piepjohn (2003) assume an Eocene age of deformation for northern and eastern North Greenland, associated with the Eurekan Orogeny.

The Trolle Land Fault System borders the Harder Fjord Fault Zone, but cross-cutting relationships remain unclear. Lyberis and Manby (2001) observed that the Harder Fjord Fault Zone cuts off the Trolle Land Fault Zone, the outermost fault of the Trolle Land Fault System (Fig. 7a), whereas von Gosen and Piepjohn (2003) report continuity of the two fault systems, with faults of the Trolle Land Fault System bending to follow an east-west trend, parallel to the Harder Fjord Fault Zone.

3 Material and Methods

3.1 Material

Samples from Johannes V. Jensen Land and Hans Egede Land were collected during expedition PS115/1 of the German research icebreaker Polarstern in 2018 (MZ-prefix). Additional samples from Herluf Trolle Land and Kronprins Christian Land were collected during the CASE 20 expedition, organized by the German Federal Institute for Geosciences and Natural Resources (BGR; CXX-prefix). Finally, we included legacy samples provided by the BGR rock repository, collected from Nyeboe Land, the Frigg Fjord Area and Lockwood Island during the CASE 2 expedition in 1994 (SE- and HP-prefixes). As at that time GPS was not available, the sample coordinates as reported in Tables 1 and 2 were manually picked from the CASE 2 field maps.

The majority of the samples are mid to Late Cretaceous magmatic and sedimentary rocks, including the "greenstones", for which a Late Cretaceous intrusion age is assumed but not yet proven. Furthermore, we analysed Proterozoic to Cambrian basement rocks including samples from the Midtkap igneous suite (Estrada et al., 2018; Rosa et al., 2016) and (meta-)sedimentary rocks from the Franklinian Basin. Two samples are from the Triassic succession of the Wandel Sea Basin and one from a mineralized fault of unknown age within the Harder Fjord Fault Zone (Tables 1 and 2).

https://doi.org/10.5194/egusphere-2026-1389
Preprint. Discussion started: 25 March 2026

Table 1: Results of AFT analysis.

Sample	n[1]	ΣNs[2]	ΣΩ[3] [µm²]	ΣP[4]	U (±SD) [ppm]	pooled Age ±1σ [Ma]	central Age ±1σ [Ma]	P(χ)²	MSWD	MTL [µm] (n)[5]	av. Dpar [µm]
MZ18-54	Johannes V. Jensen Land, *83°20.53'N 28°42.63'W 1214 m*, conglomeratic sandstone, Cambro-Ordovician										
	40	553	86953	4.35	183.8 (±733.0)	46 ± 4	52 ± 6	0	7.7	14.3 ± 1.7 (40)	2.2
MZ18-55	Johannes V. Jensen Land, *83°12.64'N 27°58.93'W 10 m*, Polkorridoren Group: conglomeratic sandstone, Cambrian										
	10	247	28199	1.90	58.6 (±58.8)	40 ± 8	40 ± 10	<0.1	8	14.3 ± 1.4 (24)	2
MZ18-56	Johannes V. Jensen Land, *83°25.6'N 27°3.05'W 1322 m*, conglomeratic sandstone, Cambro-Ordovician										
	30	484	90950	3.04	183.8 (±733.0)	41 ± 4	45 ± 4	0	2.2	14.3 ± 1.4 (115)	2.1
MZ18-57	Johannes V. Jensen Land, *83°23.71'N 25°34.75'W 10 m*, conglomeratic meta-sandstone, Cambro-Ordovician										
	35	623	100370.9	3.54	19.6 (±20.3)	48 ± 4	50 ± 3	0	2.1	14.2 ± 1.0 (105)	2
MZ18-58	Hans Egede Land, *83°7.229'N 26°30.907'W 20 m*, 'undivided sediements': mylonitic schist, Upper Proterozoic - lower Paleozoic										
	9	303	36886.7	0.68	14.5 (±40.4)	83 ± 10	195 ± 74	<0.1	3.9	13.8 ± 1.3 (28)	1.8
MZ18-60	Hans Egede Land, *83°7.475'N 24°30.525'W 30 m*, Paradisfjeld Group: schist, Cambrian										
	36	481	110754	5.58	29.7 (±26.3)	26 ± 3	28 ± 3	<0.1	4.1	14.1 ± 1.5 (75)	2.1
HP31	Frigg Fjord, *picked from field map: 83°10.41884'N 34°45.78695'W 120 m*, dolerite, Upper Cretaceous										
	17	62	38682.7	1.12	16.6 (±26.8)	23 ± 6	29 ± 4	0.11	1.4	14.3 ± 0.7 (17)	1.7
HP38	Frigg Fjord, *picked from field map: 83°10.29001'N 33°24.907'W 206 m*, float stone: greywacke, ?										
	40	882	147210	5.06	28.0 (±20.4)	39 ± 3	30 ± 2	0.21	1.2	14.4 ± 1.1 (138)	1.9
HP40	Frigg Fjord, *picked from field map: 83°10.26667'N 33°30.7468'W 160 m*, mineralized fault, age unknown										
	14	21	53610	0.18	1.4 (±2.3)	26 ± 13	39 ± 9	0.53	0.9	14.4 ± 1.1 (64)	1.8
SE2A	Frigg Fjord, *picked from field map: 83°12.79968'N 34°14.48192'W 160 m,* dolerite, Upper Cretaceous										
	40	50	149820	0.21	0.8 (±0.5)	53 ± 16	63 ± 9	1	0.2	14.3 ± 1.4 (67)	2.5
SE7	Frigg Fjord, picked from field map: *83°12.78071'N 33°10.74658'W 667 m*, basalt, Upper Cretaceous										
	40	510	94970	1.42	7.9 (±15.8)	155 ± 17	96 ± 14	<0.1	3	14.3 ± 1.4 (64)	2.2
SE20	Frigg Fjord, *picked from field map: 83° 11.974'N 34° 16.875'W 159 m,* 'greenstone', Upper Cretaceous										
	40	59	145350	0.27	1.1 (±0.2)	49 ± 27	64 ± 8	1	0.3	14.2 ± 1.4 (65)	2.2
SE22	Frigg Fjord, *picked from field map: 83° 11.974'N 34° 16.875'W 159 m,* 'greenstone', Upper Cretaceous										
	37	64	153120	0.26	1.6 (±2.5)	49 ± 21	60 ± 7	1	0.3	13.7 ± 1.5 (69)	2.2
SE39	Nyeboe Land, *picked from field map: 83°9.68001'N 31°22.2971'W 451 m*, Midtkap igneous suite: granite, Cambrian										
	12	1298	28630	1.65	30.7 (±24.3)	265 ± 17	266 ± 11	0.73	0.7	13.9 ± 1.2 (32)	2.1
SE141	Nyeboe Land, *picked from field map: 83°10.74344'N 31°36.71713'W 409 m,* Midtkap igneous suite: diorite, Neoproterozoic										
	20	3177	109630	1.55	16.3 (±6.2)	298 ± 15	303 ± 12	<0.1	5.3	14.6 ± 1.1 (143)	2.8
SE50	Lockwood Ø, *picked from field map: 83°22.5957'N 40°25.26032'W 70 m*, granite in basalt, Upper Cretaceous										
	35	379	113110	1.99	11.5 (±14.6)	41 ± 4	42 ± 3	0.75	0.8	14.1 ± 1.4 (165)	2.4
SE87	Lockwood Ø, *picked from field map: 83°21.09321'N 40°3.09101'W 190 m,* Kap Washington Group: greywacke, Upper Cretaceous										
	40	96	166670	0.39	1.9 (±2.0)	49 ± 10	56 ± 6	1	0.5	13.8 ± 1.4 (209)	2.1
CXX-34	Herluf Trolle Land, *82° 44.257´N 21° 34.705'W 314 m*, Herlufsholm Strand Fm: medium sandstone, Upper Cretaceous										
	39	366	118371	5.14	44.3 (±57.4)	21 ± 3	25 ± 4	0	4.6	14.2 ± 1.4 (115)	1.9
CXX-35	Herluf Trolle Land, *82° 44.257´N 21° 34.705'W 314 m*, Herlufsholm Strand Fm: medium sandstone, Upper Cretaceous										
	37	411	89364	6.15	57.4 (±71.2)	22 ± 3	25 ± 2	0	2	14.2 ± 1.5 (57)	2
CXX-37	Herluf Trolle Land, *82° 40.575´N 21° 09.861´W 655 m*, Dunken Fm: coarse sandstone, Triassic										
	8	187	21162	0.87	20.0 (±14.1)	58 ± 9	52 ± 9	0	5.3	14.0 ± 1.4 (23)	2.4
CXX-42	Kap Rigsdagen, *82° 01.184´N 21° 12.008´W* , Thyra Ö Fm: sandstone, Eocene										
	33	1206	91791	3.46	17.9 (±20.1)	104 ± 7	94 ± 29	0	11	13.4 ± 1.8 (85)	2.3
CXX-27	Kilen, *81° 13.371´N 13° 56.204'W 133 m*, Isrand Fm: fine sandstone, Triassic										
	40	774	128035.9	4.73	44.2 (±121.1)	45 ± 4	47 ±5	<0.1	1.6	14.0 ± 1.2 (107)	2.3
CXX-30	Kilen, *81° 21.340´N 14° 06.373'W 383 m*, Galadriel Fjeld Fm, Hondal member: sandstone, Middel Cretaceous										
	40	530	114689.1	3.43	26.4 (±54.5)	47 ± 4	47 ± 9	<0.1	3.3	14.0 ± 1.5 (112)	2
CXX-31	Kilen, *81° 19.682´N 14° 01.243'W 361 m*, Galadriel Fjeld Fm, Hondal member: sandstone, Middel Cretaceous										
	40	930	152400.3	4.87	24.6 (±28.2)	46 ± 3	51 ± 6	<0.1	2.1	13.7 ± 1.2 (101)	2
CXX-14	Amdrup Land, *80° 59.287´N 15° 18.336'W 316 m*, Independence Fjord Fm: metasandstone, Paleoproterozoic										
	30	1782	145119.7	1.10	7.7 (±3.1)	272 ± 16	278 ± 23	<0.1	2.8	13.5 ± 1.5 (114)	2
CXX-25	Amdrup Land, *80° 55.144´N 17° 12.973'W 600 m*, Hougaard Ø Fm: phyllite, Paleoproterozoic										
	40	346	118571.6	0.32	2.8 (±8.0)	288 ± 32	304 ± 32	0.67	0.9	14.0 ± 1.5 (105)	2.2

[1]n = number of counted grains with U composition > 0.1 ppm

[2]ΣNs = sum of counted spontaneous tracks in analysed grains

[3]ΣΩ [µm²] = sum of area with counted tracks in analysed grains, for comparison: laser spot size 20 µm - ablated area ~314 µm²

[4]ΣP = sum of individual 238U/43Ca ratios of analysed grain areas

[5]MTL [µm] (n) = mean track length ± standard deviation (number of measured tracks)

235

https://doi.org/10.5194/egusphere-2026-1389
Preprint. Discussion started: 25 March 2026

Table 2: Results of AHe thermochronolgy.

Sample		U	Th	Sm	He	TAE[1]	raw Age	eU[2]	Rs[3]	Ft[4]	N ter[5]	corrected Age	± error
		[ppm]	[ppm]	[ppm]	[ncc]	[%]	[Ma]	[ppm]	[µm]			[Ma]	[Ma]*
MZ18-52	Herluf Trolle Land, *82° 51.133'N 22°17.441'W 850 m*, Independence Fjord Fm: coarse-grained sandstone, Paleoproterozoic												
	#1	94.9	6.7	41.0	1.494	0.6	25	97	51	0.68	1	37	2
	#2	45.8	3.7	16.7	1.192	1.7	41	47	39	0.59	1	69	4
	#3	29.1	5.4	38.7	1.571	11.0	20	31	40	0.60	1	33	4
	#4	43.3	1.2	39.1	2.084	8.8	19	44	49	0.68	2	28	3
MZ18-54	Johannes V. Jensen Land, *83°20.53'N 28°42.63'W 1214 m*, conglomeratic sandstone, Cambro-Ordovician												
	#1	6.9	84.7	20.7	0.105	0.9	11	27	54	0.68	0	16	1
	#2	3.9	22.2	6.9	0.046	1.5	27	9	48	0.63	0	42	2
	#3	25.2	12.1	26.8	0.225	0.5	22	28	74	0.78	1	28	1
MZ18-55	Johannes V. Jensen Land, *83°12.64'N 27°58.93'W 10 m*, Polkorridoren Group: conglomeratic sandstone, Cambrian												
	#1	14.6	8.4	32.7	0.122	1.4	40	17	44	0.64	2	62	3
	#2	31.1	3.8	21.3	0.469	0.7	51	32	51	0.69	2	74	4
	#3	19.5	10.6	9.2	0.228	1.2	50	22	46	0.65	2	77	4
	#4	2.1	9.5	29.1	0.043	1.7	35	4	51	0.67	2	52	3
	#5	19.7	49.8	74.0	0.315	0.5	40	32	45	0.63	2	64	3
MZ18-56	Johannes V. Jensen Land, *83°25.6'N 27°3.05'W 1322 m*, conglomeratic sandstone, Cambro-Ordovician												
	#1	5.0	121.2	65.3	0.278	0.8	66	33	39	0.54	2	123	6
	#2	15.1	10.7	31.5	0.086	1.3	38	18	39	0.59	2	64	3
MZ18-58	Hans Egede Land, *83°7.229'N 26°30.907'W 20 m*, 'undivided sediments': mylonitic schist, Upper Proterozoic - lower Paleozoic												
	#1	0.2	1.8	3.2	0.017	3.6	87	1	56	0.69	0	125	8
	#2	0.0	1.4	4.2	0.019	2.6	170	0	57	0.68	0	247	14
	#3	0.4	8.5	6.8	0.021	2.1	28	2	55	0.68	0	41	2
MZ18-60	Hans Egede Land, *83°7.475'N 24°30.525'W 30 m*, Paradisfjeld Group: schist, Cambrian												
	#1	2.2	4.4	15.3	0.080	1.3	60	3	58	0.72	2	83	4
	#2	6.8	3.1	15.8	0.159	2.0	84	8	50	0.69	0	121	7
	#3	4.8	15.6	18.5	0.218	0.9	81	9	53	0.68	2	119	6
	#4	46.8	3.1	30.7	0.951	0.8	56	48	76	0.79	1	71	4
HP13	Frigg Fjord, *picked from field map: 83°12.80655'N 33°12.18706'W 659 m*, greywacke, Upper Cretaceous												
	#1	*18.9*	*38.5*	*52.0*	*0.452*	*2.3*	*351*	*28*	*37*	*0.55*	*1*	*622*	*34*
	#2	25.0	78.7	30.4	0.051	1.5	15	43	45	0.62	1	25	1
	#3	15.5	63.7	32.0	0.035	1.3	16	30	43	0.61	1	27	1
HP40	Frigg Fjord, *picked from field map: 83°10.26667'N 33°30.7468'W 160 m*, mineralized fault, age unknown												
	#1	0.2	1.0	2.2	0.002	3.9	15	0	57	0.69	0	22	1
	#2	1.3	2.1	2.2	0.011	3.6	10	2	66	0.75	2	13	1
SE2A	Frigg Fjord, *picked from field map: 83°12.79968'N 34°14.48192'W 160 m,* dolerite, Upper Cretaceous												
	#1	*0.7*	*4.7*	*22.7*	*0.057*	*1.9*	*114*	*2*	*46*	*0.66*	*0*	*171*	*9*
	#2	0.7	3.6	21.9	0.022	2.1	39	2	56	0.71	0	54	3
	#3	*0.8*	*3.1*	*17.5*	*0.041*	*1.9*	*105*	*2*	*51*	*0.68*	*0*	*152*	*8*
	#4	1.4	5.5	28.1	0.029	1.7	23	3	54	0.71	0	32	2
	#5	0.8	3.0	18.6	0.016	2.5	42	2	48	0.67	0	63	4
SE18B	Frigg Fjord, *picked from field map: 83° 11.974'N 34° 16.875'W 159 m,* 'greenstone', Upper Cretaceous												
	#1	1.2	4.7	26.6	0.032	2.4	50	2	48	0.67	0	74	4
	#2	2.0	7.8	35.2	0.040	1.3	23	4	59	0.73	0	31	2
	#3	1.3	5.3	24.1	0.029	2.0	37	3	55	0.70	0	53	3
	#4	1.0	3.8	21.7	0.018	2.8	35	2	50	0.68	0	51	3
	#5	1.4	4.6	26.8	0.016	2.7	26	3	47	0.66	0	39	2
	#6	3.8	15.6	60.6	0.031	1.9	20	8	49	0.65	1	31	2

https://doi.org/10.5194/egusphere-2026-1389
Preprint. Discussion started: 25 March 2026

Table 2: Continued.

Sample		U	Th	Sm	He	TAE[1]	raw Age	eU[2]	Rs[3]	Ft[4]	N ter[5]	corrected Age	± error
		[ppm]	[ppm]	[ppm]	[ncc]	[%]	[Ma]	[ppm]	[µm]			[Ma]	[Ma]*
SE19	Frigg Fjord, *picked from field map: 83° 11.974'N 34° 16.875'W 159 m,* 'greenstone', Upper Cretaceous												
	#1	1.4	5.4	25.2	0.028	1.9	25	3	56	0.72	0	34	2
	#2	1.3	4.6	23.2	0.028	1.9	58	3	47	0.65	0	88	5
	#3	*1.1*	*4.6*	*21.8*	*0.090*	*1.4*	*169*	*2*	*50*	*0.67*	*0*	*249*	*13*
	#4	1.0	3.6	21.8	0.017	3.1	47	2	45	0.64	0	72	4
	#5	*0.7*	*3.1*	*16.7*	*0.123*	*1.9*	*155*	*2*	*65*	*0.75*	*0*	*206*	*11*
	#6	2.9	10.2	50.4	0.103	1.2	36	5	74	0.78	1	46	2
SE20	Frigg Fjord, *picked from field map: 83° 11.974'N 34° 16.875'W 159 m,* 'greenstone', Upper Cretaceous												
	#1	1.8	7.0	38.3	0.034	1.3	27	4	59	0.71	1	37	2
	#2	1.0	4.6	25.7	0.022	1.7	50	2	44	0.64	0	78	4
	#3	1.3	4.8	28.2	0.031	1.3	28	3	54	0.71	0	39	2
	#4	1.0	4.1	23.8	0.012	3.0	29	2	48	0.66	0	43	3
	#5	1.4	4.8	25.5	0.013	3.1	22	3	47	0.66	0	33	2
	#6	2.5	9.5	49.1	0.014	3.4	23	5	48	0.66	1	34	2
SE22	Frigg Fjord, *picked from field map: 83° 11.974'N 34° 16.875'W 159 m,* 'greenstone', Upper Cretaceous												
	#1	0.9	3.8	20.4	0.028	1.3	35	2	59	0.73	0	47	2
	#2	0.7	2.8	16.0	0.021	2.0	33	1	60	0.73	0	45	2
	#3	*1.3*	*7.2*	*25.4*	*0.119*	*1.3*	*89*	*3*	*62*	*0.73*	*0*	*122*	*6*
	#4	1.5	5.6	28.5	0.036	2.5	57	3	49	0.66	0	84	5
	#5	1.1	5.0	23.9	0.016	3.8	24	2	52	0.68	0	35	2
SE23	Frigg Fjord, *picked from field map: 83° 11.974'N 34° 16.875'W 159 m,* 'greenstone', Upper Cretaceous												
	#1	1.8	8.3	38.3	0.034	1.9	49	4	44	0.63	0	77	4
SE132	Nyeboe Land, *picked from field map: 83°9.68001'N 31°22.29719'W 451 m,* float stone: dolerite, ?												
	#1	0.8	3.3	19.3	0.025	3.2	95	2	43	0.62	0	151	9
	#2	1.0	4.3	21.0	0.027	2.4	99	2	42	0.60	0	162	9
	#3	1.3	4.4	20.8	0.008	5.9	34	2	39	0.56	0	60	5
	#4	1.1	4.9	22.2	0.054	2.1	197	2	40	0.58	0	331	18
SE139	Nyeboe Land, *picked from field map: 83°10.41054'N 32°1.65312'W 859 m,* floatstone: gabbro, ?												
	#1	1.2	5.5	33.2	0.029	3.0	29	3	58	0.72	0	40	2
	#2	1.0	4.5	37.6	0.007	2.2	25	2	45	0.63	1	39	2
	#3	0.5	2.9	16.8	0.024	2.0	40	1	61	0.73	0	54	3
	#4	0.5	2.2	19.7	0.026	2.3	61	1	56	0.72	0	84	5
	#5	0.8	3.9	26.4	0.024	2.1	41	2	57	0.71	0	56	3
SE141	Nyeboe Land, *picked from field map: 83°10.74344'N 31°36.71713'W 409 m,* Midtkap igneous suite: diorite, Neoproterozoic												
	#1	35.6	69.3	12.5	0.397	0.7	40	52	56	0.70	1	58	3
	#2	28.3	45.8	8.6	0.903	0.6	53	39	60	0.73	0	72	4
	#3	20.4	41.2	12.2	0.662	0.5	40	30	63	0.73	2	54	3
	#4	37.0	72.3	9.2	0.918	0.7	43	54	57	0.71	2	61	3
	#5	28.5	48.2	11.8	0.729	0.4	43	40	59	0.72	2	60	3
	#6	37.2	72.6	12.2	0.384	0.6	42	54	43	0.61	2	69	3
SE47	Lockwood Ø, *picked from field map: 83°21.7648'N 40°23.63673'W 380 m,* Kap Washington Group: rhyolitic breccia, Upper Cretaceous												
	#1	*1.1*	*5.4*	*37.1*	*0.127*	*2.9*	*278*	*3*	*52*	*0.68*	*1*	*401*	*23*
	#2	1.1	5.8	32.0	0.025	2.4	32	3	51	0.69	0	46	3
SE50	Lockwood Ø, *picked from field map: 83°22.5957'N 40°25.26032'W 70 m* , granite in basalt, Upper Cretaceous												
	#1	1.6	6.9	20.7	0.021	1.6	23	3	52	0.68	0	33	2
	#2	1.4	4.6	21.2	0.008	3.5	24	3	43	0.61	0	39	2
	#3	1.3	4.9	19.9	0.008	4.3	23	3	43	0.61	0	38	2
	#4	1.3	5.4	18.7	0.018	2.3	28	3	50	0.67	1	42	2
	#5	1.3	5.8	24.1	0.011	3.0	28	3	41	0.60	0	46	3

https://doi.org/10.5194/egusphere-2026-1389
Preprint. Discussion started: 25 March 2026

Table 2: Continued.

Sample		U [ppm]	Th [ppm]	Sm [ppm]	He [ncc]	TAE[1] [%]	raw Age [Ma]	eU[2] [ppm]	Rs[3] [µm]	Ft[4]	N ter[5]	corrected Age [Ma]	± error [Ma]*
SE87	Lockwood Ø, *picked from field map: 83°21.09321'N 40°3.09101'W 190 m,* Kap Washington Group: greywacke, Upper Cretaceous												
	#1	2.4	18.9	19.0	0.046	1.6	26	7	49	0.66	0	40	2
	#2	2.1	13.2	37.3	0.087	1.4	29	5	66	0.75	0	38	2
	#4	2.7	16.8	38.1	0.067	1.1	47	7	55	0.68	1	68	3
	#5	2.1	10.1	35.7	0.035	2.1	36	5	48	0.65	0	55	3
	#6	1.9	13.3	13.2	0.101	1.4	36	5	67	0.74	0	48	2
CXX-34	Herluf Trolle Land, *82° 44.257´N 21° 34.705'W 314 m* , Herlufsholm Strand Fm: medium sandstone, Upper Cretaceous												
	#1	15.3	34.8	62.2	0.104	0.8	15	24	55	0.69	1	22	1
	#2	6.3	12.9	28.6	0.052	0.9	19	9	51	0.69	0	27	1
	#3	4.8	13.6	34.4	0.084	0.9	20	8	65	0.75	0	27	1
	#4	32.2	59.9	86.0	0.040	1.5	12	47	41	0.60	1	20	1
CXX-35	Herluf Trolle Land, *82° 44.257´N 21° 34.705'W 314 m* , Herlufsholm Strand Fm: medium sandstone, Upper Cretaceous												
	#1	54.8	96.9	57.1	0.158	0.9	25	78	42	0.61	1	40	2
	#2	36.8	41.6	55.2	0.207	1.4	22	47	53	0.69	1	33	2
CXX-30	Kilen, *81° 21.340´N 14° 06.373'W 383 m* , Galadriel Fjeld Fm, Hondal member: sandstone, Middel Cretaceous												
	#3	17.8	71.6	60.2	0.135	0.8	27	35	43	0.60	0	46	2
CXX-31	Kilen, *81° 19.682´N 14° 01.243'W 361 m* , Galadriel Fjeld Fm, Hondal member: sandstone, Middel Cretaceous												
	#2	62.7	18.0	42.1	0.248	0.9	26	67	41	0.61	2	43	2
	#3	1.1	66.9	27.9	0.061	1.1	31	17	55	0.67	1	47	2
	#4	15.7	92.5	14.6	0.409	1.5	34	37	54	0.68	2	50	3
CXX-14	Amdrup Land, *80° 59.287´N 15° 18.336'W 316 m* , Independence Fjord Fm: metasandstone, Paleoproterozoic												
	#1	20.5	1.2	5.5	2.191	0.7	205	21	62	0.74	2	274	14
	#2	4.9	0.1	2.2	0.128	1.5	46	5	64	0.75	2	62	3
	#3	4.8	0.9	2.8	0.164	1.3	55	5	66	0.76	2	72	4
	#4	5.1	1.6	2.3	0.049	1.3	28	6	54	0.71	2	39	2
	#5	2.4	0.4	1.5	0.013	3.5	35	3	50	0.68	1	51	3
	#6	3.5	0.1	1.4	0.089	2.1	40	4	67	0.77	2	53	3
CXX-20	Amdrup Land, *80° 58.903´N 15° 18.789'W 352 m* , migmatitic gneiss, Paleoproterozoic												
	#1	0.7	0.4	5.7	0.014	3.1	47	1	57	0.72	1	65	4
	#2	0.6	0.5	3.3	0.020	12.2	50	1	64	0.75	2	67	9
	#3	0.7	0.2	3.8	0.024	4.5	38	1	78	0.80	0	48	3
	#4	0.6	0.2	4.3	0.008	4.0	37	1	53	0.70	2	53	3
	#5	0.7	1.2	3.6	0.207	3.1	229	1	87	0.81	1	282	17
CXX-25	Amdrup Land, *80° 55.144´N 17° 12.973'W 600 m* , Hougaard Ø Fm: phyllite, Paleoproterozoic												
	#1	0.4	2.4	26.8	0.038	1.5	209	1	43	0.64	0	318	17
	#2	0.9	3.8	31.3	0.059	2.8	145	2	45	0.65	0	219	13
	#3	0.5	2.7	28.2	0.054	1.8	170	1	48	0.68	0	246	13
CXX-26	Amdrup Land, *80° 55.144´N 17° 12.973'W 600 m* , Hougaard Ø Fm: metasandstone, Paleoproterozoic												
	#1	51.4	19.2	17.5	0.261	0.5	18	56	50	0.68	2	26	1
	#2	13.1	9.1	40.4	0.070	1.6	21	15	58	0.72	1	29	1
	#3	25.1	14.4	16.0	0.651	1.2	125	29	43	0.63	2	198	10
	#4	3.8	14.0	34.0	0.181	1.4	168	7	53	0.68	1	245	13
	#5	12.3	2.8	11.9	0.741	1.8	413	13	43	0.62	0	650	35

[1]TAE = total analytical error

[2]eU = effective Uranium content, calculated as $eU = U + 0.235Th + 0.0053Sm$

[3]Rs = equivalent sphere radius

[4]Ft = α-ejection correction

[5]N ter = number of terminations of the analysed grain

*Ft-correction with 5% error and TAE

https://doi.org/10.5194/egusphere-2026-1389
Preprint. Discussion started: 25 March 2026

3.2 Methods

Please use only the styles of this template (MS title, Authors, Affiliations, Correspondence, Normal for your text, and Headings 1–3). All rocks were crushed and processed using standard heavy mineral separation methods, for obtaining apatite separates. Details of rock processing are described in the Supporting Information. We applied fission track and (U-Th-Sm)/He thermochronology for all samples which yielded sufficient or suitable apatite. Additionally, we undertook apatite U-Pb analysis on two samples from the "greenstones" (SE20 & SE22), for testing the assumed Late Cretaceous intrusion ages. Apatite U-Pb, fission track and (U-Th-Sm)/He thermochronology are all temperature- dependent radiometric dating methods. Apatite U-Pb is based on the radioactive decay of U to stable Pb. The apatite U-Pb system is sensitive to temperatures between 570 °C and 350°C (Cherniak, 2010; Cochrane et al., 2014). Apatite Fission Track (AFT) thermochronology is based on damages of the crystal lattice, caused by the spontaneous decay of U, which accumulate over time. It is most sensitive to temperatures between 60 °C and 120 °C (Wagner et al., 1989). Apatite (U-Th-Sm)/He (AHe) thermochronology is based on the accumulation of radiogenic He in the crystal lattice, resulting from the alpha-decay of U, Th and Sm. It is most sensitive to temperatures between 40 °C and 85 °C (Wolf et al., 1998).

Apatite U-Pb analyses were carried out using a Photon Machines Iridia 193nm UV laser ablation (LA) system with a Cobalt two–volume cell coupled to an Agilent 7900 quadrupole inductively coupled plasma mass spectrometer (ICP–MS) at Department of Geology, Trinity College Dublin. The sample aerosol was transported by a flow of helium carrier gas (0.45 L/min) and was subsequently mixed with argon (0.6 L/min) and N2 (9 mL/min) before entering the plasma torch. For all analyses of apatite reference materials and unknowns, a repetition rate of 13 Hz, a spot size of 50 µm and a fluence of 2.5 J/cm2 was employed, with each analysis lasting 27 s followed by a 9 s background measurement. The raw isotope data were reduced using the "VizualAge UcomPbine" data reduction scheme of Chew et al. (2014) within the IOLITE package of Paton et al. (2011). AFT analyses were performed by GeoSep Services, using laser-ablation inductively coupled plasma mass spectrometry as described by Donelick et al. (2005) and Hasebe et al. (2004). Mounted apatites were etched with 5.5 M HNO3 for 20 s. Central ages were calculated with IsoplotR (Vermeesch, 2018) using single grain ages with U > 0.1 ppm. Prior to track length measurements, 252Cf irradiation was applied. Dpar values were measured for kinetic information. AHe analysis was carried out at the University of Bremen, using whole grain digestion. Raw ages were corrected for alpha ejection (Farley et al., 1996) incorporating the stopping distance of Ketcham et al. (2011). The resulting AHe ages were assessed for the influences of radiation damage, grain size in relation to usage of broken grains and Helium implantation (Fig S2, Beucher et al., 2013; Brown et al., 2013; Shuster et al., 2006; Spiegel et al., 2009). Details on the analytical procedures are described in the Supporting Information.

AFT and AHe data were integrated by thermal history inversions, which provide time-temperature paths in agreement with the data observed (e.g., Ketcham, 2005). For this, we used the following strategy: (1) Independent information such as sedimentary histories and organic maturation data were included as constraints (listed in Table S2); (2) We tried to obtain similar cooling patterns for samples located close to each other. Strongly contrasting thermal histories were interpreted as

https://doi.org/10.5194/egusphere-2026-1389
Preprint. Discussion started: 25 March 2026

indications for differential movements and hence for fault activity; (3) We tested for all samples whether their cooling histories are in agreement with the four cooling episodes described for the Eurekan Belt as exposed in northern Ellesmere Island (Vamvaka et al., 2019).

For testing and complementing our own thermal history inversions, we assessed previously published, statistically robust AFT data from North Greenland in our study (Japsen et al., 2021, 2023; we defined «statistically robust» as AFT central ages based on n >15 single grain ages; Table S4). These data were originally modelled without clear descriptions and justifications of the included constraints, and by using an unpublished and inaccessible annealing algorithm. The published thermal models cannot be directly compared to our models, but we assessed whether the documented cooling phases would be in agreement with the cooling phases of Vamvaka et al. (2019). Insufficient documentation of key parameters prevented inverse remodelling. We chose to forwardly remodel one sample of the published data according to the strategy described above, which is located at a key structural position to our samples (sample GC1113-3, Fig.3).

Moreover, we remodelled AFT and AHe data from a set of Late Cretaceous sandstones from the Nakkehoved area. These data and their models were published previously (Meier et al., 2024). Since then, new data has become available which show that the sedimentary rocks from Nakkehoved contain zircons with U-Pb ages of ~70 Ma (Guarnieri et al., 2025a, b), constraining their depositional ages to ≤70 Ma. We included this information in new thermal history inversions. The resulting time-temperature paths provide more precise thermal histories than those previously published.

Our models were performed by the HeFTy software, using a Monte Carlo approach (Ketcham, 2005). They utilized c-axis projections (Ketcham et al., 2007a), the fission track annealing algorithm of Ketcham et al. (2007b), and Dpar as kinetic indicator (e.g. Donelick, 1993). AHe dates were integrated with the AFT data or – when no AFT data were available - modelled alone, using the stopping distances and alpha correction of Ketcham et al. (2011) and two different diffusion models (Farley, 2000; Flowers et al., 2009). The fit between the predicted data and the data observed is assessed using the Goodness of Fit (GOF) value, with GOF-values >0.5 indicating a good statistical fit, and GOF-values >0.05 indicating an acceptable statistical fit (Ketcham, 2005). All details are described in the Supporting Information.

4 Results

4.1 Results of apatite U-Pb analysis

The two “greenstone“ samples (SE20, SE22) yielded Tera-Wasserburg U-Pb lower intercept ages (anchored using a 207Pb/206Pb initial ratio derived from the Stacey and Kramers (1975) terrestrial Pb evolution model) of 81±5 and 77±6 Ma, that is, overlapping within uncertainty limits (Fig. 3). These ages, which we interpret as intrusion or near-intrusion ages, are within the same range as previously analysed unmetamorphosed mafic dykes from North Greenland (Thórarinsson et al., 2015).

https://doi.org/10.5194/egusphere-2026-1389
Preprint. Discussion started: 25 March 2026

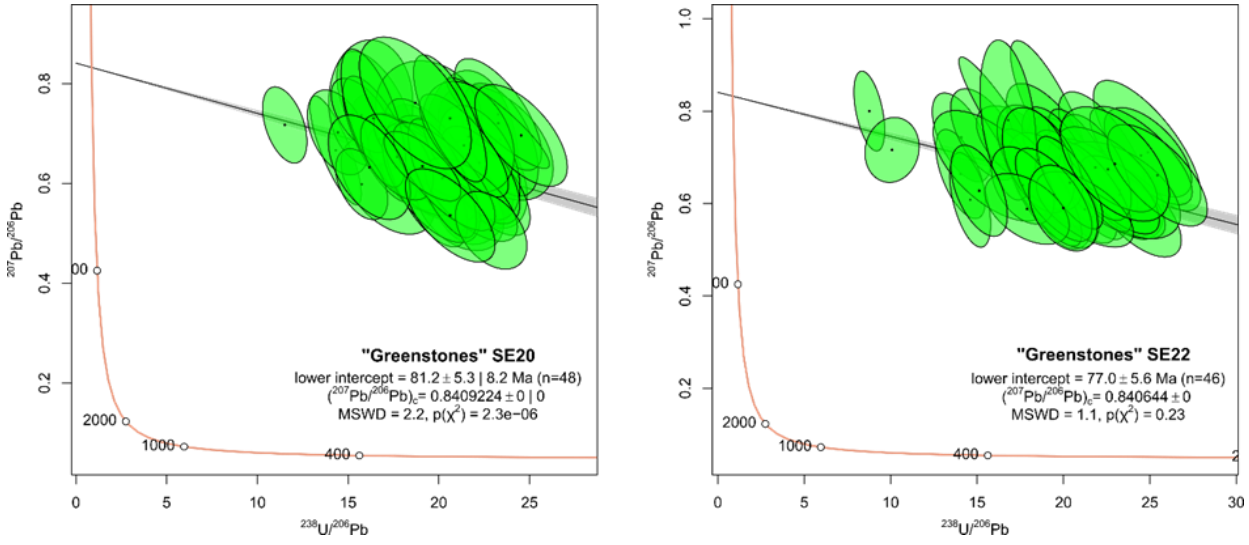

Figure 3: Tera-Wasserburg U-Pb lower intercept ages of the 'greenstones' samples SE20 and SE22 (anchored using a 207Pb/206Pb initial ratio derived from the Stacey and Kramers (1975) terrestrial Pb evolution model).

4.2 Results of apatite fission track and (U-Th-Sm)/He analysis

AFT ages and mean track lengths were obtained from twenty-six samples (Table 1). AFT central ages range between 25 ± 4 Ma and 304 ± 32 Ma, mean track lengths range between 13.4 and 14.6 µm (reported here without c-axis projection) with average Dpar values between 1.7 and 2.8 µm. No distinct kinetic populations based on Dpar values were identified. As expected, the basaltic lithologies contained apatite with low U-concentrations, leading to larger uncertainties as compared to other lithologies. AHe ages were obtained from twenty-eight samples. The results are shown in Table 2. The AHe ages range between 13 ± 1 and 318 ± 17 Ma. The majority of AHe dates are younger than the associated AFT dates. However, for some samples we observe cross-over relationships, that is, contrary to what would be expected due to the lower closure temperature, AHe dates are older than the AFT age of the same sample. No systematic ages-elevation relationship is detected and the age distribution across North Greenland does not show obvious spatial trends. However, the following generalisations can be made:

(1) In northernmost North Greenland (Johannes V. Jensen Land, Lockwood Island), AFT and AHe ages are between 33 and 52 Ma (i.e., within the time range of the Eurekan deformation) or younger, with no clear age-elevation relationships (samples SE47, SE50, SE87, MZ18-54, MZ18-56, MZ18-57).

(2) The "greenstones" within the Harder Fjord Fault Zone and dolerite in close vicinity yielded AFT dates between 60 and 64 Ma (samples SE2A, SE20, SE22).

(3) The samples with AFT dates between195 and 304 Ma are derived from within the Harder Fjord Fault Zone and toward the western boundary of the Trolle Land Fault System and contain AHe dates between 39 and 72 Ma (samples MZ18-58, SE39, SE141, CXX-14, CXX-25).

https://doi.org/10.5194/egusphere-2026-1389
Preprint. Discussion started: 25 March 2026

(4) With the exception of sample HP31, the youngest AFT dates between 25 and 28 Ma occur along the eastern coast (samples MZ18-60, CXX-34, CXX-35).

(5) AHe dates with cross-over relationships are all derived from deformed samples associated with fault zones (samples MZ18-55, MZ18-56, MZ18-58 MZ18-60, CXX-35, SE87, SE22).

(6) In eastern North Greenland (Herluf Trolle Land, Kilen), AFT and AHe dates are between 43 and 52 Ma, within the time range of Eurekan deformation (samples CXX-37, CXX-27, CXX-30, CXX-31).

4.3 Results of thermal history modelling

As described in the "Methods" section (Section 3.2.), our modelling strategy aims to develop a general model for all samples constrained by independent geological information (e.g. deposition/crystallisation age, vitrinite reflectance) and spatial coherence between neighbouring samples and to test whether the cooling phases in pre-Eurekan (66-60 Ma), Eurekan I (55-48 Ma), Eurekan II (44-38) and post-Eurekan (34-26 Ma) observed on the Pearya terrane of northern Ellesmere Island (Vamvaka et al. 2019) are consistent with the data from North Greenland.

The thermal history models support that all of the four cooling phases are also present in North Greenland, but without any obvious spatial trend (Fig. 4b-d, Fig. 5b, Fig. 6b, Fig. 7c). In several places, samples in close spatial vicinity (of less than 10 km) show different thermal histories. The evaluation of the cooling phases of the individual samples from Japsen et al. (2021, 2023) are broadly consistent with the cooling phases supported by our thermal history models.

In general, Greenland north of the Harder Fjord Fault Zone has experienced significant cooling during the Cenozoic, while within the fault zones cooling varies between minor to extensive during the Cenozoic. For the Trolle Land Fault System, Cenozoic cooling is strongest in the northeast and declines towards southwest, except for the Nakkehoved area in the northeast, where cooling occurred in the latest Cretaceous. In contrast to Japsen et al. (2021, 2023) our thermal history models support Palaeogene cooling in Amdrup Land. The cooling pattern inferred from our thermochronological data follows the pattern of deformation described for the Trolle Land Fault system that is focussed on the Kilen area and the outermost Herluf Trolle Land and declining towards the NE and SW in Kronprins Christian Land (Pedersen and Håkansson, 2001; Zinck-Jørgensen, 1994a, b).

5 Discussion

5.1 The late Cretaceous evolution of North Greenland

The Cretaceous period set the stage for the subsequent changes in the early Cenozoic, such as the formation of the intraplate Eurekan Belt, the opening of the northern North Atlantic Ocean, and the opening of the Eurasia Basin widening the Arctic Ocean. Yet the late Cretaceous tectonic and sedimentary evolution of the Arctic is still poorly understood as the sedimentary record is limited in North Greenland to only patchy, mostly fault-bound remnants of Cretaceous deposits and lacking completely on Svalbard (Smelror and Larssen, 2016). Our study includes several samples with Cretaceous deposition or

https://doi.org/10.5194/egusphere-2026-1389
Preprint. Discussion started: 25 March 2026

intrusion ages and hence provide additional data for reconstruction the Cretaceous evolution. Our observations and inferences are summarized as follows:

(1) AFT and AHe dates of Cretaceous sedimentary rocks vary significantly, but they all postdate their depositional ages, in agreement with varying but generally high vitrinite reflectance values >1% reported for the Upper Cretaceous sequences of North Greenland (Fig. 4a, Håkansson et al., 1994; Paech and Estrada, 2019). Resetting of the AFT system was also reported from previously analysed Upper Cretaceous samples (Japsen et al., 2021) and hence seems to be the rule rather than the exception, indicating that the Upper Cretaceous strata in North Greenland experienced temperatures >120 °C post deposition. The timing of maximum heating is best constrained by the remodelled samples from the Nakkehoved area, previously interpreted as an allochthonous terrane originally situated closer to the Kap Washington area at the northern margin of North Greenland (Meier et al., 2024). These samples have depositional ages ≤70 Ma (U-Pb ages of detrital zircons; Guarnieri et al., 2025a, b) and experienced post-depositional heating to temperatures >250 °C (indicated by vitrinite reflectance values between 7 and 10 %, Håkansson et al., 1994), and have cooled to temperatures below ~120 °C by ~68 to 65 Ma (indicated by thermal history modelling, Fig. 4b). This brackets the timing of maximum heating between 70 and ~65 Ma.

A similar timing is obtained from sedimentary rocks from the Kap Washington Group, to which Nakkehoved, according to the interpretation as an allochthonous terrane, was likely close during the Cretaceous: Sample SE87 was deposited during the Maastrichtian (Thórarinsson et al., 2011a), subsequently heated, and already cooled during the Palaeocene, constraining the timing of heating to latest Cretaceous to earliest Palaeocene (Fig. 4c).

Other Cretaceous sedimentary rocks of this study experienced a main cooling phase during the Eurekan or post-Eurekan, with the timing of maximum heating being loosely constrained between mid to late Cretaceous deposition and Eocene or Oligocene cooling. However, their thermal histories do not exclude maximum heating at 65-70 Ma, contemporaneous with the Nakkehoved samples. This is also in agreement with previous suggestions for the Kilen area, where maximum heating was suggested to have occurred between the Santonian and the Palaeocene – Eocene (Pedersen et al., 2018).

(2) AFT and AHe ages of all Cretaceous magmatic rocks analysed in this study postdate their intrusion ages. Only the basaltic sample from the Frigg Fjord area (SE7) yielded an AFT age close to the intrusion age of the mafic dykes from North Greenland (Fig. 4a, Thórarinsson et al., 2015).

Of particular interest for constraining the Cretaceous thermal history are the “greenstone” samples with Late Cretaceous intrusion ages (77 and 81 Ma, Fig. 3) and AFT ages of 64 - 60 Ma (Table 1). This supports previous suggestions that the “greenstones“ of the Harder Fjord Fault Zone are the deformed equivalents of the unmetamorphosed Late Cretaceous dykes exposed outside the Harder Fjord Fault Zone (Estrada, 2000). Subsequent to the intrusion, these rocks were affected by hydrothermal alteration, associated with the growth of minor quantities of secondary minerals, amongst others, chlorite, biotite, green and brown amphibole and epidote (Estrada, 2000, Table S3). This suggests temperatures of ca. 350 °C. Furthermore, the dyke rocks show intense mechanical fragmentation and display slickensides. Our thermal history models show that by ~65 Ma, the” greenstones” have already cooled to temperatures <120 °C (Fig. 4d), which in turn implies a thermal overprint after Late Cretaceous intrusion and prior to ~65 Ma, which coincides with the heating of the Nakkehoved sedimentary samples.

https://doi.org/10.5194/egusphere-2026-1389
Preprint. Discussion started: 25 March 2026

In summary, consistent heating of Late Cretaceous samples across whole North Greenland suggests that the northern continental margin was subsiding and being buried during the Late Cretaceous, forming a connected and extended sedimentary basin from the Kap Washington area in the north to Kronprins Christian Land in eastern North Greenland (Fig. 4e). This basin must have been subjected to a strongly enhanced heat flow between ~70 and 65 Ma, as preserved in the "greenstones" and in the Nakkehoved and Kap Washington sedimentary rocks, followed by pronounced exhumation that lasted until ~60 Ma. The latter event is also recorded on adjacent Ellesmere Island (Vamvaka et al., 2019).

Previously, the Cretaceous strata of North Greenland were interpreted as isolated occurrences deposited in small independent basins which are thought to have developed in response to pull-apart movements ('Kilen Event', Håkansson et al., 1991; Håkansson and Pedersen, 2015; Håkansson and Stemmerik, 1995). This interpretation was based on the different depositional facies from terrestrial (Kap Washington), to fluviatile (Depot Bugt, Herluf Trolle Land) to marine (Frigg Fjord/Santon glacier, Kilen, Nakkehoved) over a relative short distance (cf. Håkansson et al., 1991). However, we suggest that the different sedimentary environments may be due to fault-controlled segmentation of a larger basin, causing topographic highs and lows with varying water depths and deposition rates. This scenario is in agreement with the variable vitrinite reflectance values reported in the literature (Håkansson et al., 1994; Paech and Estrada, 2019) and also supports the suggestion of Piepjohn and von Gosen (2001) who postulated a wider cover of Upper Cretaceous sediments, rather than deposition within small independent basins based on the correlatable, well-sorted and fine-grained character of the Upper Cretaceous silt- and sandstones deposits along the Harder Fjord Fault Zone and Trolle Land Fault System. Recent fieldwork in Kilen enabled correlation of the Sølverbæk Fm with the Kveite Formation on the Barents Shelf (Hovikoski et al., 2018) and suggests that further equivalents of the Upper Cretaceous deposits might also be found on the Barents shelf (Svennevig et al., 2017).

As the large-scale tectonic environment is a segmented basin with enhanced and locally strongly variable heat flow, we speculatively suggest that the North Greenland margin may have formed the eastern continuation of a continental rift basin. Such a basin was recently postulated to have formed along the northern margin of Ellef Ringnes, Axel Heiberg and Ellesmere Islands during the Late Cretaceous to early Cenozoic (Stephenson and Anudu, 2025). This scenario would be in agreement with the rift-related intra-plate geochemical signatures reported for the basaltic dykes (Estrada, 2000; Estrada et al., 2001; Soper et al., 1982; Thórarinsson et al., 2015), and in particular with the east-west strike of the "greenstones" and some other dykes (the slightly earlier to contemporaneous N-S and slightly older NW-SE striking dykes of North Greenland, in contrast, have been associated with rifting along the Gakkel Ridge and of the Labrador Sea-Baffin Bay , respectively (Døssing et al., 2013; Thórarinsson et al., 2015)). During Eurekan tectonics, the Cretaceous basin became dissected and most of the basin was eroded, except isolated occurrences preserved within fault zones.

https://doi.org/10.5194/egusphere-2026-1389
Preprint. Discussion started: 25 March 2026

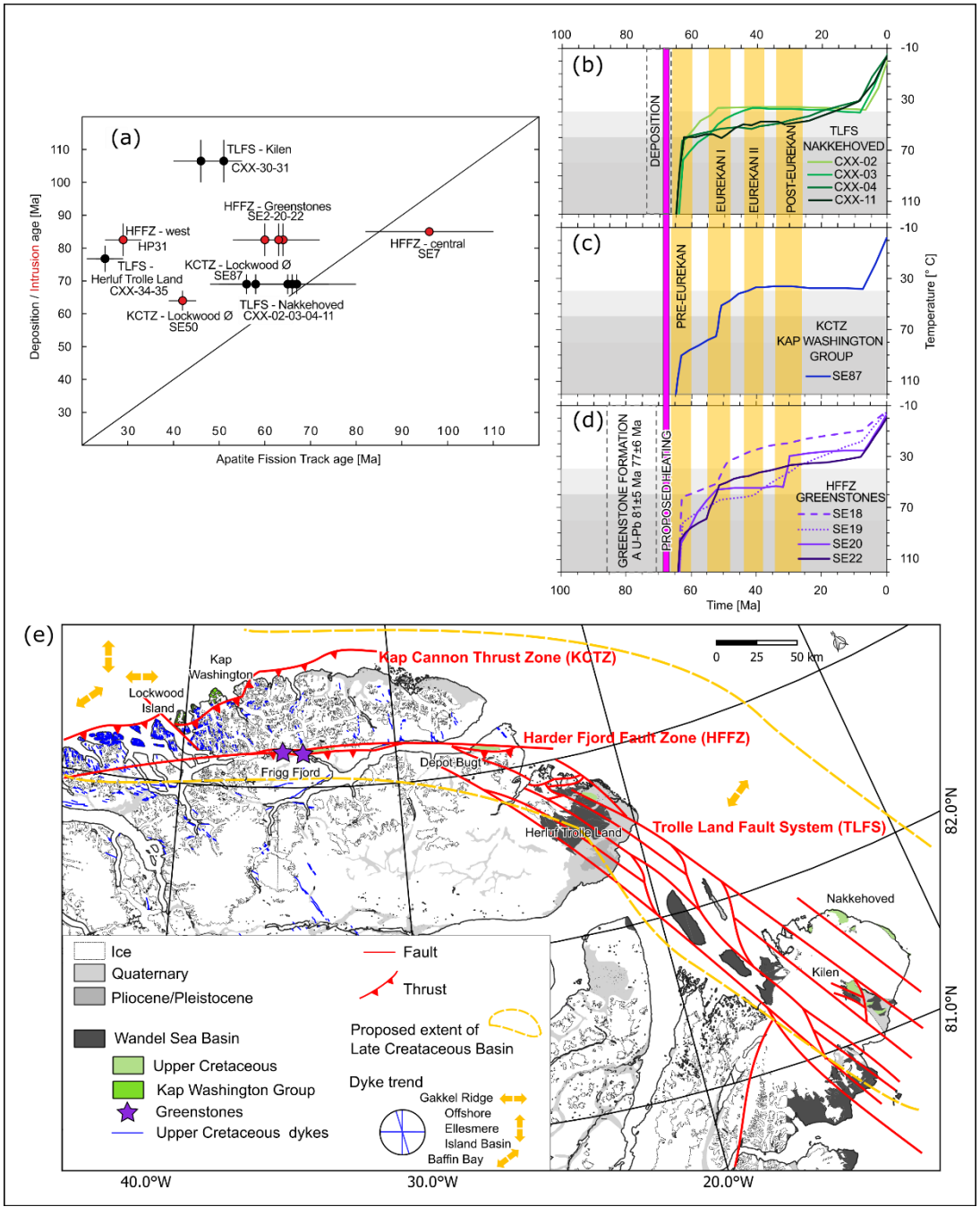

Figure 4: Indications for the existence of a Late Cretaceous basin on the north-eastern margin of North Greenland. (a) AFT ages plotted against deposition/intrusion age showing resetting in AFT ages of Late Cretaceous deposits, consistent with increased temperatures indicated by vitrinite reflectance data. (b)-(d) Mean paths of the thermal history models constraining the timing of proposed heating to 70-65 Ma. (e) Map showing the proposed minimum extent of a Late Cretaceous basin associated dyke emplacement and Kap Washington volcanism (modified from Kokfelt et al. 2023 and Piepjohn et al. 2016).

https://doi.org/10.5194/egusphere-2026-1389
Preprint. Discussion started: 25 March 2026

5.2 Relationships between the main Eurekan fault systems of North Greenland

The non-systematic distribution of the thermochronological ages in North Greenland, which are unrelated to age-elevation relationships, and the contrasting thermal histories of neighbouring samples in close vicinity can only be explained by complex fault patterns. By comparing the thermal histories of the individual fault-delimited tectonic blocks, the timing of fault activities can be inferred, contributing to a better understanding of the kinematic, temporal and spatial relationship of the Eurekan fault systems.

5.2.1 Kap Cannon Thrust Zone

We assessed activity on the Kap Cannon Thrust Zone along a N-S section across the three different tectonic blocks of Lockwood Island (Fig. 5). For the southern block, we had to rely on remodelling of data published by Japsen et al. (2021). This model is unfortunately associated with high uncertainties, as it lacks AHe and track length data. The thermal history models from the central block (SE87) and the northern block (SE50) are much better constrained, as they are based on AFT ages and lengths, combined with AHe data.

During the Palaeocene pre-Eurekan period, the central block has already exhumed into the temperature range of the sensitivity of AFT system, that is <120° C. The two other blocks were at temperatures >120°C, so that their potential movements are not recorded by AFT or AHe thermochronology (Fig. 5b, c). However, the displacement of the central block relative to the northern and southern blocks suggests pre-Eurekan activity along both the Kap Cannon Thrust and the Kap Christiansen Fault. This is also in agreement with Palaeocene Ar-Ar mica ages from the mylonites of the southern block, as reported by Lyberis and Manby (2001) and Manby (2014) from the Kap Cannon and Kap Washington area.

During the Eurekan I (early Eocene), the central block continued to cool, while the northern and southern blocks remained at temperatures >120° C (Fig. 5b, c), suggesting tectonic activity along the two faults bordering the central block. The northern block experienced major cooling during the Eurekan II (late Eocene), nearly juxtaposing the present structural levels of the central and the northern blocks (Fig. 3c) and witnessing a tectonically active Kap Christiansen Fault. The limited data from the southern block also suggest a main exhumation phase during Eurekan II and hence activity of the Kap Cannon Thrust can be inferred.

During the post-Eurekan (Oligocene), the northern block again experienced cooling, whereas the central block was stagnant, suggesting renewed activity of the Kap Christiansen Fault. The limited resolution of the model from the southern block does not allow inferences for post-Eurekan fault movement on the Kap Cannon Thrust.

https://doi.org/10.5194/egusphere-2026-1389
Preprint. Discussion started: 25 March 2026

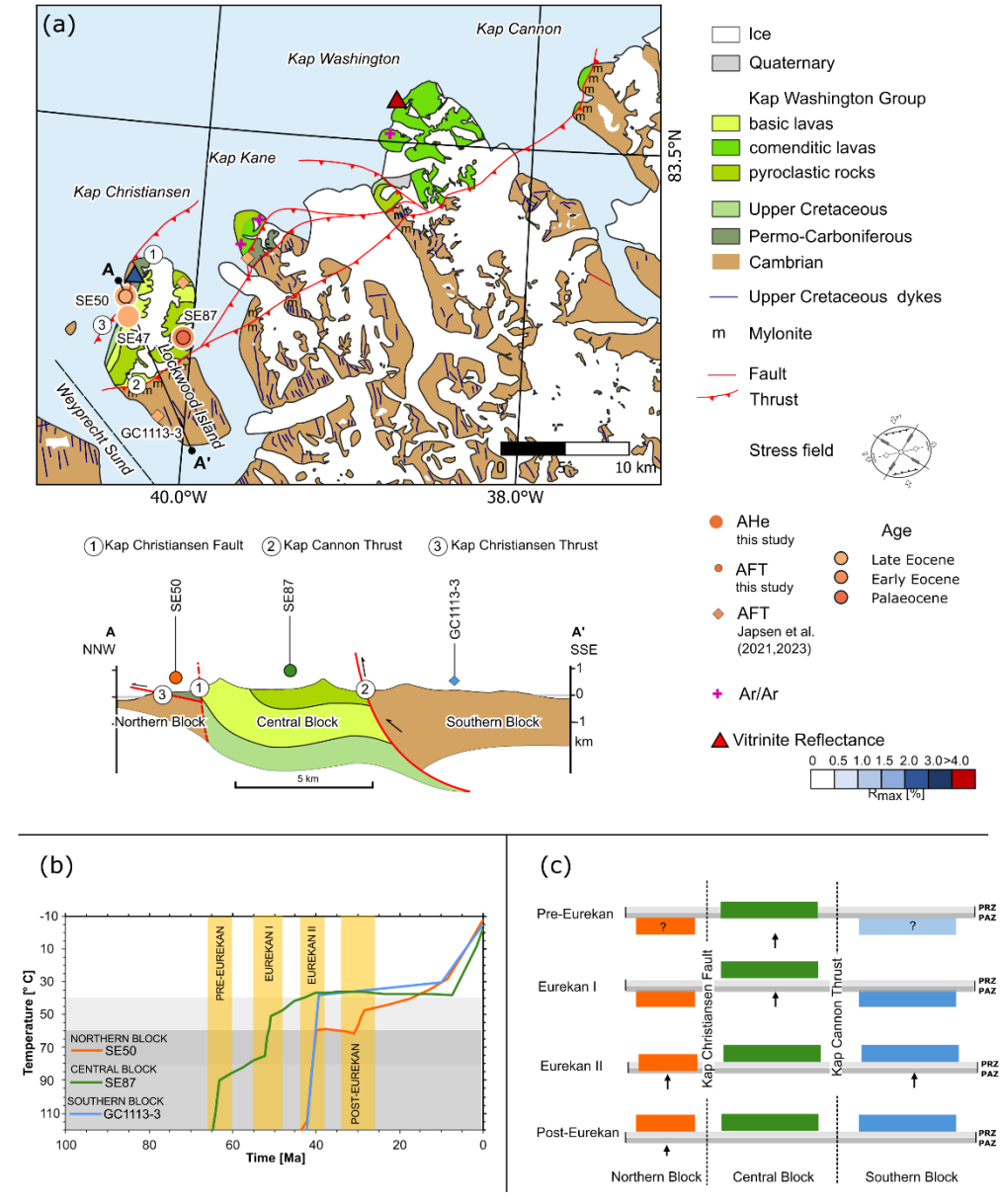

455

Figure 5: Thermochronological results and the thermal evolution of the crustal blocks of Lockwood Island. (a) Geological map showing the extent of the Kap Washington Group (Kokfelt et al., 2023; Soper and Higgins, 1991), new and published thermochronological data (this study, Japsen et al., 2021, 2023, Table S4) vitrinite reflectance data (Paech & Estrada, 2019), published Ar-Ar ages (Estrada et al., 2001; Tegner et al., 2011) and the structure of the Kap Cannon Thrust Zone with a profile
460 **section across Lockwood Island (von Gosen and Piepjohn, 1999). (b) Mean paths of the thermal history models for the Northern, Central and Southern blocks indicating activity in the Kap Christiansen Fault and Kap Cannon thrust. (c) Schematic block diagrams illustrating the contrasting exhumation of the Northern, Central and Southern blocks and associated fault activity during the pre-Eurekan, Eurekan I and II and post-Eurekan.**

https://doi.org/10.5194/egusphere-2026-1389
Preprint. Discussion started: 25 March 2026

5.2.2 Harder Fjord Fault Zone

The varying thermal histories suggest complex differential movements of the single blocks within the Harder Fjord Fault Zone. We utilized the mapped faults within the Harder Fjord Fault Zone (e.g., Kokfelt et al., 2023; Pedersen, 1980) to delineate and define individual blocks with common thermal histories, assuming that the fault closest to the sample represents the border of a tectonic block (Fig. 6). We are aware that, given the low data density and the complex fault patterns, this approach is a strong simplification. However, we consider it as a viable way to gain overarching information on the structural evolution, which can be refined by future studies. Based on this approach we draw the following conclusions:

(1) The core area of the Harder Fjord Fault Zone is formed by a –presumably contiguous– block that sits to both sides of the Frederick E. Hyde Fjord (including samples SE39, SE141 and MZ18-58, coloured in violet in Fig. 6a, and termed "Old Core" in the following text). This block was already at temperatures of ~50 °C prior to the Eurekan and experienced final cooling below 40 °C during the Palaeocene pre-Eurekan (Fig. 6b). This shows that the tectonic mélange of the Harder Fjord Fault Zone comprises parts which remained at very shallow crustal levels throughout the Cenozoic and which were nearly unaffected by Eurekan exhumation within the sensitivity of the applied low-temperature thermochronometers (Fig. 6c).

(2) In contrast, the "Greenstone Block" (in green, samples: SE02, SE20, SE22) shows major cooling below 120°C in the pre-Eurekan, and additional cooling during Eurekan I (Fig. 6b). The Greenstone Block is separated from the static Old Core by a set of northwest-southeast trending faults. The contrasting cooling behaviour of the two blocks suggests that one or several of these faults were active during the Palaeogene and during the early Eocene.

(3) The "Northern Basement Block" (in blue: MZ18-54, MZ18-56, MZ18-57) cooled mainly during Eurekan I and Eurekan II, while the adjacent sample MZ18-55 differs from this pattern and exhibits main cooling during Eurekan II, suggesting that it is separated from the Northern Basement Block by a fault. Such a fault has not been identified in the field but satellite imagery shows a northwest-southeast-trending lineament, parallel to mapped faults, which we postulate as a fault that cuts off MZ18-55 from the Northern Basement Block and that was active during late Eocene Eurekan II (see Fig. S5 of Supporting Information).

(4) Also during Eurekan II, the "Southern Basement Block" (in turquoise: HP38, HP40) was exhumed. It is separated from the static Greenstone Block and the Old Core by east-west and by northwest-southeast trending faults, respectively, suggesting that these structures were active during the late Eocene.

(5) Finally, during the Oligocene post-Eurekan, the "Triangle Block" (in pink: MZ18-60) experienced pronounced cooling. It is separated from the Northern Basement Block by the apparently fault-controlled southwest-northeast trending part of the Frederick E. Hyde Fjord and from the Old Core by approximately east-west trending structures. Both fault sets seem to have been active during the Oligocene. Moreover, the "Western Basement Block" (in dark green: HP31) was exhumed during the post-Eurekan, neighbouring the "Old Core" and the "Greenstone Block" along the northwest-southeast trending Frigg Fjord (which we again interpret as following a fault) and along an east-west trending fault, respectively. The Greenstone Block may

https://doi.org/10.5194/egusphere-2026-1389
Preprint. Discussion started: 25 March 2026

have also experienced some minor cooling during the Oligocene, but not as pronounced as the adjacent Western Basement Block.

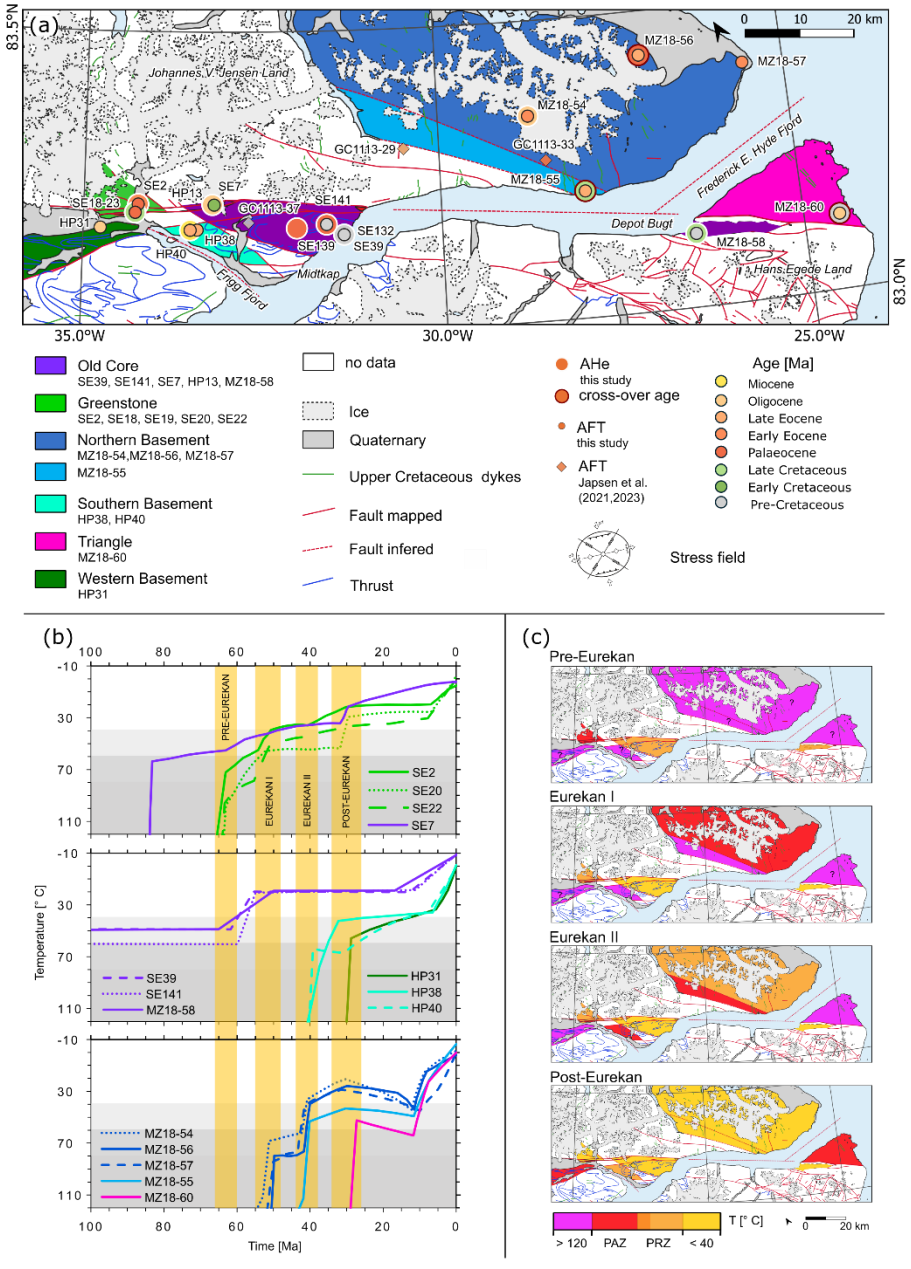

Figure 6: Thermochronological data and resulting thermal history evolution of samples from the Harder Fjord Fault Zone. (a) Extent of the Harder Fjord Fault Zone and its associated faults and stress field, with crustal blocks differentiated by their thermal history (faults modified from Kokfelt et al., 2023). Sample locations and results of new and published thermochronological data are shown (this study; Japsen et al., 2021 data in Table S4), (b) Mean paths of the thermal history models of the respective crustal blocks showing cooling during the pre-Eurekan, Eurekan I and II and post-Eurekan. (c) Schematic block-scale thermal evolution illustrating differential exhumation and inferred fault activity during the preEurekan, Eurekan I and II and post-Eurekan.

https://doi.org/10.5194/egusphere-2026-1389
Preprint. Discussion started: 25 March 2026

5.2.3 Trolle Land Fault System

This fault system comprises several large dextral strike-slip faults which dissect Kronprins Christian and Herluf Trolle Land into five major blocks (Fig. 7a,b). Several smaller faults further segment these major blocks, but they are difficult to trace due to ice, water and Quaternary deposit cover, and are largely neglected here.

Sample CXX-25 from the basement southwest of the Trolle Land Fault System yields pre-Cenozoic cooling signatures. Its thermal history suggests that it remained close to the surface during the Eurekan, confirming previous observations that Eurekan deformation is restricted to the area of the Trolle Land Fault System (Stemmerik et al., 2000). During Eurekan I, Amdrup Land shows moderate exhumation (cooling signatures were not attributed to the Eurekan by previous studies without AHe data, such as Japsen et al. (2021, 2023)). Simultaneously with the moderate exhumation of Amdrup Land, Kilen and its equivalent block in Herluf Trolle Land (Block IV) were subject to pronounced exhumation (Fig. 7c). This observation is in agreement (1) with increasing deformation of the margins of the Trolle Land Fault System towards the Kilen Block, as reported by Pedersen and Håkansson (2001), and (2) with early Eocene activity on faults separating Amdrup Land from the Kilen Block, accommodating variable amounts of exhumation between these two blocks. Erosion of these exhuming blocks may have sourced the late Palaeocene to early-middle Eocene sediments of the Thyra Ø Formation, deposited in pull-apart basins between Kronprins Christian Land and Herluf Trolle Land (i.e., the Princess Islands, Fig. 7a).

While the Amdrup Land Block remained static during Eurekan II, the Kilen Block and its equivalent on Herluf Trolle Land (Block IV) continued to exhume, suggesting activity of the fault(s) in between. The formerly subsiding Princess Islands also became involved in Eurekan tectonics (Piepjohn et al., 2025) and started to exhume during Eurekan II (Meier et al., 2024). Due to the lack of data sensitive to lower temperatures than the AFT system, previous studies did not resolve the two different episodes of Eurekan exhumation in the Trolle Land Fault System, but assumed a single cooling period during the latest Eocene (Japsen et al., 2021, 2023).

Finally, Block V of Herluf Trolle Land experienced pronounced exhumation during the post-Eurekan, presumably accommodated by movements along the fault between Blocks IV and V (Fig. 7c). No data is available from the equivalent to Block V in Kronprins Christian Land (that is, the block between Kilen and Nakkehoved). The easternmost, coastal part of Kronprins Christian Land is formed by the Nakkehoved Block, which shows major cooling during the pre-Eurekan and hence a distinctly different thermal history compared to the coastal area of Herluf Trolle Land (i.e., Block V). However, Nakkehoved was previously described as an allochthonous terrane originally situated much further north (Meier et al., 2024), and hence its cooling history may not be representative for the Trolle Land Fault System.

https://doi.org/10.5194/egusphere-2026-1389
Preprint. Discussion started: 25 March 2026

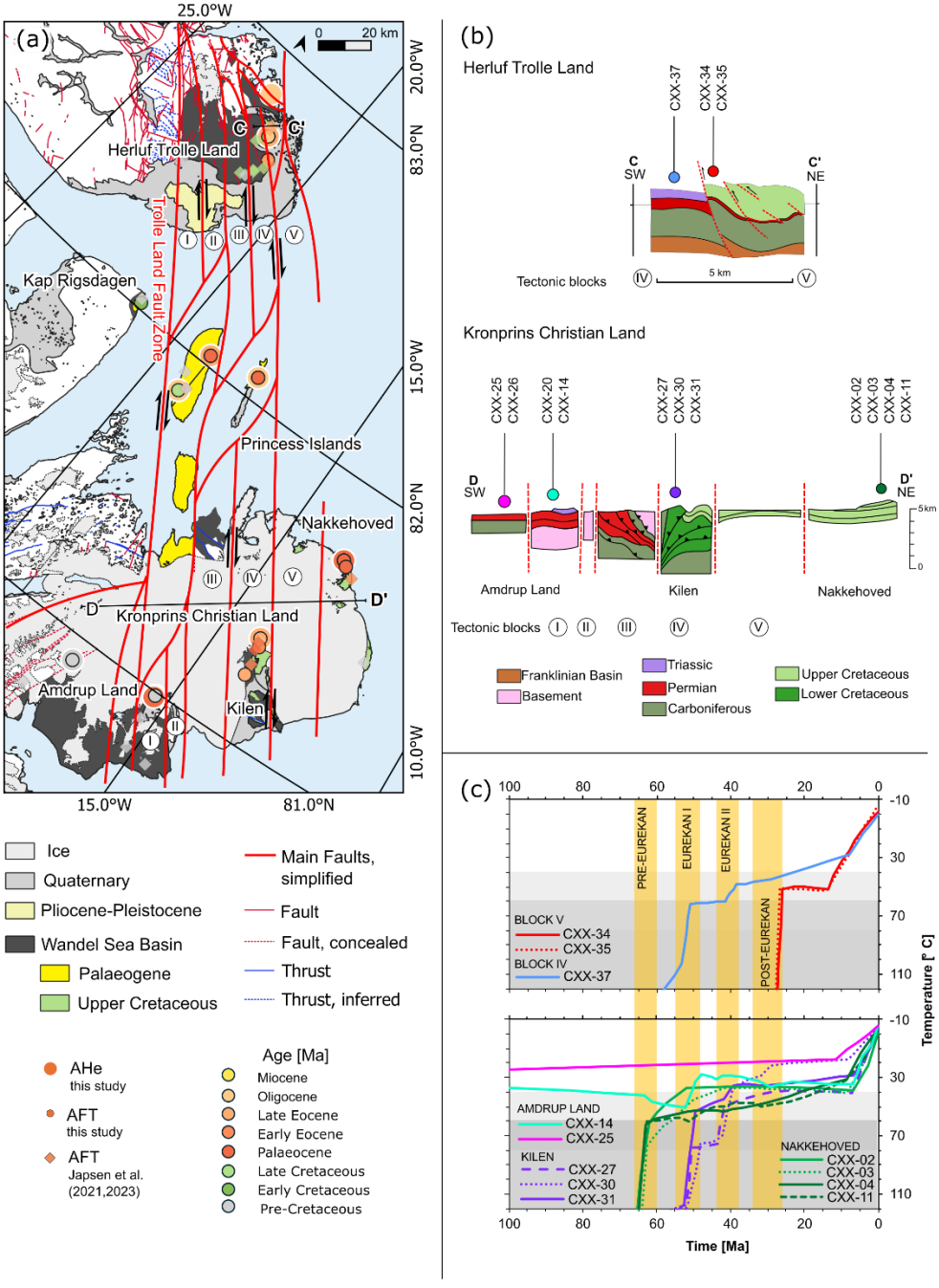

Figure 7: Results of thermochronology and thermal history modelling in relation to tectonic blocks of the Trolle Land Fault System. (a) Geological map showing the Trolle Land Fault System and the crustal blocks in Herluf Trolle Land and Kronprins Christian Land (modified from Kokfelt et al., 2023; Piepjohn et al., 2016) with new and published thermochronological data (this study; Japsen et al., 2021, 2023; Meier et al., 2024). (b) Structural profiles across block IV and V in Herluf Trolle Land (top, after Zinck-Jørgensen, 1994a) and across the crustal blocks of Kronprins Christian Land (bottom, after Pedersen and Håkansson, 2001), with sample locations indicated. (c) Mean paths of the thermal history models for the respective samples, showing pronounced cooling during Eurekan I and II and the post Eurekan.

https://doi.org/10.5194/egusphere-2026-1389
Preprint. Discussion started: 25 March 2026

5.2.4 Synchronous activity and interaction of North Greenland's major fault systems

The faults within the Kap Cannon Thrust Zone, the Harder Fjord Fault Zone, and the Trolle Land Fault System were all episodically active during Eurekan I and II as well as during the post-Eurekan, and probably also during the pre-Eurekan. Therefore, our findings confirm contemporaneous activity of all three larger fault systems, arguing in favour of the models of von Gosen and Piepjohn (2003). Furthermore, their contemporaneous movements imply that all three fault zones were connected and interacted with each other, as postulated by Håkansson and Pedersen (1982). In particular, the Harder Fjord Fault Zone accommodated simultaneous activity of differently oriented faults. Our data are in agreement with the following scenario:

The fault systems in northern and eastern North Greenland constitute a coherent transform fault system with a main northwest-southeast direction, and with associated conjugate faults. The contemporaneous exhumation of the crustal blocks in the fault zones suggest that associated differently-orientated faults were active in response to the prevailing stress field. The Eurekan stress field, causing north-south compression along the Kap Cannon Thrust Zone, corresponds to the stress field identified for reverse faulting along the Harder Fjord Fault Zone and to the stress field associated with the dextral transpression observed in the Trolle Land Fault System (von Gosen and Piepjohn, 1999, 2003; Guarnieri, 2015; Lyberis and Manby, 2001; Piepjohn and von Gosen, 2001). This further implies that the Harder Fjord Fault Zone and the Trolle Land Fault System do not intersect but conjugate, and movements between both fault systems are compensated and transferred through the east-west structures. Earlier observations that northwest-southeast-trending faults merge with east-west trending faults (von Gosen and Piepjohn, 2003; Zinck-Jørgensen, 1994b) and that crustal blocks in the vicinity were rotated (Buggisch et al., 2001) are consistent with our interpretation. According to previous field observations, the Trolle Land Fault Zone, bordering the Trolle Land Fault System to the west, seems to merge into the Harder Fjord Fault Zone in the area of Frigg Fjord and may propagate to the west north of the Harder Fjord Fault Zone (Pedersen and Håkansson, 2001; Stijl and Mosher, 1998). The variations seen in the thermochronological data suggests the presence of additional, yet unmapped, associated faults, and that North Greenland represents a mosaic of crustal blocks. In summary, our findings support the model that the Kap Cannon Thrust Zone, the Harder Fjord Fault Zone and the Trolle Land Fault System are part of a common zone of deformation, that is, the Wandel Hav Mobile Belt (Håkansson and Pedersen, 1982; Pedersen and Håkansson, 2001).

We furthermore suggest that the combined transform fault system of Kap Cannon Thrust Zone, Harder Fjord Fault Zone and Trolle Land Fault System is part of the larger De Geer Fracture Zone (Lundin et al., 2023; Lundin and Doré, 2019; Piepjohn et al., 2016 and others). Håkansson and Pedersen (1982) already speculated that the Wandel Hav Mobile Belt probably extends offshore with a similar trend as the De Geer and Spitsbergen Fracture Zone. New magnetic, seismic and gravimetry studies support the presence of structures offshore eastern and northern North Greenland, that are assigned either to the Wandel Hav Mobile Belt or the De Geer Fracture Zone (Brotzer et al., 2022; Damaske and Estrada, 2003; Døssing et al., 2010; Jokat et al., 2016). Overall, the orientation of the spreading ridges of the Lena Trough, Molloy Ridge and Knipovich Ridge as well as their associated transforms also correspond to the trend of the Wandel Hav Mobile Belt and its conjugate faults and occupy the

https://doi.org/10.5194/egusphere-2026-1389
Preprint. Discussion started: 25 March 2026

position of the former De Geer Fracture Zone (Crane et al., 2001; Engen et al., 2008; Snow et al., 2011)(Meier et al., 2024; Paech and Estrada, 2019).

5.3 The tectonic evolution of North Greenland in a regional context

5.3.1 The latest Cretaceous (~70-66 Ma): Heating and burial but no evidence of exhumation

Our samples from Nakkehoved, the Kap Washington and the Harder Fjord Fault areas record a thermal event between 70 and 65 Ma, associated with temperatures exceeding those expected from burial alone. This heating is instead best explained by an increased and locally highly variable geothermal gradient and enhanced heat transfer along faults (Meier et al., 2024; Paech and Estrada, 2019). This, together with the coincident volcanism with intra-plate signature (Brown et al., 1987; Estrada et al., 2001; Thórarinsson et al., 2011b) and the evidence for the segmented, fault-controlled basin is typical for a continental rifting environment (cf. Brune et al., 2023). The inferred timing of the thermal event is in agreement with Maastrichtian to Palaeocene peak thermal conditions in North Greenland as reported by Guarnieri et al. (2025b). It is, however, in marked contradiction to Japsen's et al. (2023) assumption of "regional Maastrichtian exhumation" which "possibly reflects doming above the rising Iceland Plume". We consider both, Maastrichtian exhumation and Cretaceous movements associated with the Iceland Plume unlikely, because of (i) ongoing sedimentation during the Maastrichtian, e.g., in Nakkehoved, in the Kap Washington area, and also on the Audhild Peninsula of adjacent Ellesmere Island (e.g., Falcon-Lang et al., 2004) contradicting regional large-scale doming; (ii) none of our samples shows evidence for Late Cretaceous cooling. This does not completely exclude such a scenario, but makes a widespread cooling "event" unlikely; (iii) even if doming associated with the Iceland Plume would cause sufficient exhumation to be detected within the sensitivity limits of AFT thermochronology, plume-related uplift is suggested for the Palaeogene, rather than for the Maastrichtian (Barnett-Moore et al., 2018; Dam et al., 1998).

For the Trolle Land Fault System, a dominant deformation phase associated with wrench tectonics was postulated for the Late Cretaceous to Palaeocene and named the "Kronprins Christian Land Orogeny" (Håkansson and Pedersen, 2001; Manby and Lyberis, 2000). Our data, however, show that the areas most affected by deformation in the Trolle Land Fault System reveal cooling during Eurekan I and II. Pedersen et al. (2018) showed that the isotherms inferred for the thermal overprint of the Upper Cretaceous sediments at Kilen (Fig. 2E, 6) are folded, which implies that heating must have occurred prior to deformation and that after deformation the strata did not experience temperatures higher than 80 °C, which is within the sensitivity range of the thermochronometers we applied. We can therefore constrain the timing for the deformation to the Palaeocene to Eocene, supporting the conclusions of post-Cretaceous deformation (von Gosen and Piepjohn, 2003; Guarnieri, 2015; Svennevig et al., 2016). This contradicts a Late Cretaceous timing of deformation and hence makes a "Kronprins Christian Land Orogeny" unrelated to Eurekan deformation unlikely.

https://doi.org/10.5194/egusphere-2026-1389
Preprint. Discussion started: 25 March 2026

5.3.2 The Pre-Eurekan (~66-60 Ma): Extension or Convergence?

Our thermal history models from the Kap Washington area, the Nakkehoved terrane, and the Harder Fjord Fault Zone area (the "Greenstone Block") reveal a phase of pre-Eurekan exhumation between 66 and 60 Ma referring, for a conventional geothermal gradient of 30 °C/km, to the removal of at least 2.5 km to 4 km of overburden. Palaeocene exhumation of the western segment of the Eurekan Belt in Ellesmere Island was interpreted in terms of subsidence, crustal stretching, and basin formation (Vamvaka et al., 2019). To the east, in Svalbard, by contrast, Palaeocene exhumation was explained by convergence/transpression, causing, amongst others, the exhumation of Svalbard's highest peak, the Newtontoppen (Dörr et al., 2012).

North Greenland, in the centre of the Eurekan Belt, may be affected by both extension and convergence: In the Kap Washington area in the northwest of North Greenland, pre-Eurekan exhumation was accompanied by a distinct period of silicic, metaluminous magmatism, which was interpreted as reflecting –extensive– continental rifting (Thórarinsson et al., 2011b). Further east, on the other hand, Palaeocene erosion is evident by the erosional unconformities of the Depot Bugt (inferred from maturity contrast between Upper Cretaceous and Palaeogene deposits; Paech and Estrada, 2019) and within the Trolle Land Fault System. Here, the Thyra Ø Formation was deposited at the end of pre-Eurekan exhumation, that is, from the late Palaeocene onwards (Lyck and Stemmerik, 2000; Piasecki et al., 2018). At Kap Rigsdagen, the Thyra Ø Formation unconformably overlies Lower Cretaceous sediments and contains reworked Early and Late Cretaceous dinocysts (Piasecki et al., 2018). This implies that the corresponding Lower and Upper Cretaceous deposits were eroded immediately prior to the deposition of the Thyra Ø Formation and relates the unconformity to pre-Eurekan erosion. Contemporaneous early Palaeocene extension and convergence presumably refer to the same origin: The incipient opening of the Baffin Bay/ Labrador Sea (associated with extension in the west), causing Greenland to move to the northeast (resulting in contraction in the east (Fig. 1b)).

5.3.3 Eurekan I (~55-48 Ma) and Eurekan II (~44-38 Ma) – the Rise of the Eurekan Belt

Piepjohn et al. (2016) define "the Eurekan" as the phase in which Greenland moved as an independent microplate due to simultaneous spreading in the Labrador Sea/Baffin Bay and the Norwegian-Greenland Sea causing episodic deformation and exhumation (= Eurekan I and II). This definition limits the term "Eurekan" to the Eocene epoch. Other studies use "Eurekan" also in connection with earlier tectonic movements, such as the onset of spreading in the Labrador Sea or supposed Late Cretaceous movements (e.g., Gion et al., 2017; Japsen et al., 2023), which complicates comparisons between different studies. As the definition of Piepjohn et al. (2016) is based on a widely accepted and undisputed plate tectonic context (that is, the simultaneous Eocene seafloor spreading east and west of Greenland), we propose to use this definition of the Eurekan for future studies.

The amount of overburden eroded during the Eurekan in North Greenland is hard to estimate due to the locally variable geothermal gradient (cf. Meier et al., 2024) and the differential exhumation response of individual crustal blocks to tectonic

https://doi.org/10.5194/egusphere-2026-1389
Preprint. Discussion started: 25 March 2026

uplift across faults (cf. Section 5.2). Locally, removal of at least 3 km of overburden can be estimated for Eurekan I and II for a geothermal gradient of 30°C/km. This eroded material may have been deposited on the Barents Shelf, as suggested by the trace element composition of apatites in Eocene sediments on the Barents margin (Flowerdew et al., 2023).

A main difference between the exhumation phases of Eurekan I and Eurekan II is the involvement of the Palaeogene sediments in the tectonic evolution of the Eurekan Belt. During the Eurekan I, the sediments of the Eureka Sound Group on northern Ellesmere Island, of the Thyra Ø Formation in North Greenland, and of the Central Tertiary Basin on Svalbard were deposited and subsequently buried (Dörr et al., 2019b; Meier et al., 2024; Vamvaka et al., 2019). Particularly in Ellesmere Island and North Greenland, the Eurekan Belt may hence be described as a mosaic of exhuming blocks and associated subsiding syn-tectonic sedimentary basins during Eurekan I. In Svalbard, where the syn-tectonic sediments were deposited in a more defined foreland basin (i.e., the Central Tertiary Basin), the situation may have been different.

During Eurekan II, in contrast, deposition of syn-tectonic sediments ceased, the Palaeogene basins were inverted, and their infill became eroded (Barnes and Schneider, 2019; Dörr et al., 2019b; Meier et al., 2024; Vamvaka et al., 2019). In addition, deformation of the Palaeogene Thyra Ø Formation (Piepjohn et al., 2025) and the Eureka Sound Group (Piepjohn et al., 2013) shows that the sedimentary rocks became involved in Eurekan tectonics during Eurekan II. This suggests that the Eurekan Belt exhumed in a more homogenous way compared to the Eurekan I.

Our thermal histories imply a synchronous evolution of North Greenland and northern Ellesmere Island, not only with respect to the formation of the sedimentary basins, but also regarding the timing of episodic exhumation of the Eurekan Belt. Svalbard seems to have experienced a similar tectonic and geological evolution (Piepjohn et al., 2016 and references therein) but the thermochronological record from the western margin of the archipelago is still meagre.

The synchronicity of exhumation events along the Eurekan Belt implies a phase of regionally coherent tectonic activity and crustal denudation. Furthermore, based on the synchronous onset of exhumation involving the formerly subsiding sedimentary basins, we suggest that tectonic processes capable of generating surface uplift on a belt-wide scale were especially pronounced during Eurekan II. These conditions could have been favorable for topography development, even though the resulting relief may have been spatially variable, especially where erosion of weak, unlithified sediments may have dominated.

This temporal framework coincides with ice-rafted debris occurring in the sediments of the Norwegian-Greenland Sea and formation of continental ice was suggested for Greenland (Eldrett et al., 2007; Tripati and Darby, 2018; Tripati et al., 2008). Although our data do not allow us to assess the magnitude of topography formation, they provide a spatial and temporal tectonic framework within which potential interactions between Eurekan deformation, surface/crustal evolution and climate evolution can be explored. One possible scenario compatible with this framework is that ice caps nucleated on structural highs (in emerging high-relief areas) of the Eurekan Belt, while lower-altitude areas were still characterized by moderate climatic conditions and metasequoia vegetation (Jahren and Sternberg, 2008; Schouten et al., 2008; Vamvaka et al., 2019).

https://doi.org/10.5194/egusphere-2026-1389
Preprint. Discussion started: 25 March 2026

5.3.4 Post-Eurekan (~34-26 Ma): The Opening of the proto-Fram Strait?

Today, the Eurekan Belt is dissected in two segments and the gap in between is occupied by one of the most important oceanic gateways of the planet – the Fram Strait. The Fram Strait is the only deep-water connection between the Arctic Ocean and the global oceanic circulation systems. It is crucial for ventilating the Arctic Ocean, for biota exchange, and for steering the Atlantic meridional overturning circulation. The timing of the Fram Strait opening is still poorly constrained but the age of its oceanic crust, dated as between ca. 20 and 10 Ma, suggests an early to middle Miocene deep-water connection (Dumais et al., 2020; Ehlers and Jokat, 2009; Engen et al., 2008; Läderach et al., 2011). However, continental breakup and onset of seafloor spreading are usually preceded by a phase of extensional thinning of the continental crust and hence by subsidence, which may have allowed for an earlier marine connection between the Arctic and the North Atlantic oceans. The existence of such a proto-Fram Strait is discussed in the literature and was tentatively placed within the Oligocene (Gaina et al., 2025; Poirier and Hillaire-Marcel, 2011; Straume et al., 2022), but detailed radiometric dating is lacking.

Our thermal history models indicate a distinct phase of enhanced exhumation between 34 and 26 Ma, that is, after the termination of Eurekan convergent motion related to the independent movement of the Greenland plate. This post-Eurekan exhumation is particularly pronounced (but not limited to) to the coastal areas of eastern North Greenland. It is associated with activity of east-west and northwest-southeast striking faults, i.e., parallel to the North Greenland and eastern North Greenland continental margins. In agreement with Vamvaka et al. (2019), we argue that post-Eurekan exhumation was caused by a transtensional reactivation of the formerly transpressional De Geer Fracture Zone. We furthermore suggest that, as a consequence of these transtensional movements, the Eurekan Belt was dissected immediately after the end of the Eurekan Orogeny, giving way for the formation of a proto-Fram Strait from the earliest Oligocene onwards. Hence, the proto-Fram Strait may have opened along with the plate tectonic reorganizations associated with the Eocene-Oligocene boundary, that is, the cessation of spreading in the Baffin Bay/ Labrador Sea (Kristoffersen and Talwani, 1977), Greenland´s incorporation into the North American Plate (Tessensohn and Piepjohn, 2000), the resulting divergence from Eurasia (Gaina et al., 2009), and the separation of the Yermak and Morris Jesup Plateaux (Glebovsky et al., 2006).

Oligocene (trans-)tension is not limited to the coastal areas of Greenland but was of regional extent, as (1) it is also observed in northern Ellesmere Island (Vamvaka et al., 2019); (2) it is expressed by the development of horsts and graben systems west of Svalbard (Blinova et al., 2009), including the exhumation of Prins Karls Forland as a horst along the western side of the Forlandsundet Graben (Barnes and Schneider, 2019; Meier et al., 2024); (3) it is accompanied by the activity on extensional faults onshore west Spitsbergen (Haaland et al., 2024); (4) it caused the formation of the Danskøya Basin north of Svalbard (Ritzmann and Jokat, 2003), and (5) it is associated with crustal thinning of the southern Yermak Plateau (Meza-Cala et al., 2025).

Why did rapid exhumation of the post-Eurekan stop at ~26 Ma? Unlike the changes of exhumation rates during the earlier Eurekan stages, there is no obvious correlation with plate tectonic changes or changes in the rates and directions of the oceanic spreading systems. We suggest that while the regional stress field persisted, stress associated with the lateral movements

https://doi.org/10.5194/egusphere-2026-1389
Preprint. Discussion started: 25 March 2026

between Greenland and the Barents Shelf was focussed along the increasingly thinned and thermally weakened continental crust within the area of the future Fram Strait, ending the transfer of stress into the continental areas of the Eurekan Belt and hence ending resultant exhumation.

Finally, nearly all of our thermal history models suggest a poorly defined phase of enhanced exhumation from the middle to late Miocene onwards. At about the same time, at 13 Ma, faults parallel to the Forlandsundet Graben were reactivated (Haaland et al., 2024), Svalbard and North Greenland experienced exhumation associated with surface uplift (Dörr et al., 2012, 2019a; Døssing et al., 2016), and volcanism and hydrothermal activity affected North Svalbard, the Sofia Basin, the Yermak Plateau and the Morris Jesup Rise (Geissler et al., 2019; Kristoffersen et al., 2021; Meza-Cala et al., 2024; Telmon et al., 2025). Following Døssing et al. (2016), we interpret Miocene enhanced exhumation as being related to regional-scale widening of the Fram Strait between 15 and 10 Ma.

6 Conclusions

In this study, we examined the tectonic evolution of North Greenland from the Late Cretaceous through the Cenozoic with particular focus on the activity of the Eurekan fault zones and conclude the following:

1) A Late Cretaceous thermal overprint affected the margin of North Greenland, with maximum heating exceeding 120 °C between 70 and 65 Ma. This thermal event, we interpret to reflect increased geothermal gradients and burial in a Late Cretaceous rift basin and suggest crustal weakening prior to the main Eurekan deformation. The Late Cretaceous emerges as a critical phase in the tectonic evolution facilitating subsequent fracturing and deformation of the crust.

2) The Kap Cannon Thrust Zone, the Harder Fjord Fault Zone, and the Trolle Land Fault System were active during the pre-Eurekan, Eurekan I, Eurekan II, and Post-Eurekan stages. The contemporaneous reactivation of differently oriented compressional and transpressional fault systems suggests that these structures represent a coherent fault system responding to changes in the regional stress field. This coherent fault system constitutes the Wandel Hav Mobile Belt and the onshore part of the De Geer Fracture Zone. The reactivation of long-lived structures and superimposed deformation highlights the importance of crustal inheritance in intraplate orogeny.

3) The deformation in North Greenland is constrained to Palaeocene to Eocene. We estimate exhumation of at least 2.5 km during the pre-Eurekan and locally at least 3 km during the Eurekan assuming a geothermal gradient of 30°C/km, providing evidence of landscape-forming processes associated with Eurekan deformation. These results indicate the potential for topography development in North Greenland synchronous with exhumation in adjacent regions of the Eurekan Belt, including the Pearya terrane of northern Ellesmere Island.

4) Post-Eurekan exhumation in North Greenland reflects the tectonic reorganization in the northern North Atlantic and the opening of the Proto-Fram Strait. Our results support the interpretation that this gateway developed along pre-existing, long-lived structural weaknesses, emphasizing the importance of structural inheritance for margin evolution. A poorly constrained

https://doi.org/10.5194/egusphere-2026-1389
Preprint. Discussion started: 25 March 2026

phase of enhanced middle to late Miocene exhumation might be related to uplift of the North Greenland margin and volcanism offshore North Greenland and Svalbard.

Overall, this study establishes North Greenland as a key area for linking Late Cretaceous rifting, the Eurekan orogeny, and post-orogenic reorganization and for integrating the variable deformation patterns observed across the Eurekan Belt. By providing a spatial and temporal framework for fault activity and exhumation, our results define important boundary conditions for plate reconstructions and contribute to understanding the tectonic context of topographic development and environmental change in the Arctic.

Data availability

The data used in this study will be available in the Zenodo repository.

Author contributions

KM, FL and CS conceived the study. CS supervised and administrated the project. FL and CS acquired funding, KP organized the fieldwork. SE and NK provided samples and PM, POS and DC lab infrastructure and analytical expertise. KM, POS, DC and PM performed the analysis. KM, SE, NK, KP, FL and CS interpreted the results. KM modelled the data, created figures and tables and wrote the original draft of the manuscript. All authors reviewed and edited the manuscript.

Competing interests

The authors declare that they have no conflict of interest.

Acknowledgements

We thank the Federal Institute for Geosciences and Natural Resources (BGR) for financing and organising the fieldwork of the CASE and PANORAMA projects in North Greenland as well as for providing the CASE 2 samples from the National Polar Sample Repository. In this context, we would like to express our sincere gratitude to Hans-Jürgen Paech for sampling and providing field information. Further, we acknowledge the Department of Environmental Science, Aarhus University for providing logistics for Villum Research Station, where CASE 20 was based in, and thank the CASE 20 Team (Martin Blumenberg, Malte Jochmann, Antonia Ruppel, Lutz Reinhardt) for support in the field. We also like to thank the captain and crew of RV Polarstern cruise PS115/1, the helicopter crew and wildlife observers for making fieldwork possible and Maximilian Zundel for organisation and support during sample collection. For technical support we thank Anne Hübner,

https://doi.org/10.5194/egusphere-2026-1389
Preprint. Discussion started: 25 March 2026

Christiane Schott, Vera Kolb, Anke Toltz from the processing laboratory of the University of Bremen. Discussions with Peter Klitzke, Wolfram Geissler and Pierpaolo Guarnieri greatly contributed to this manuscript. KM acknowledges the State Museum of Natural History Karlsruhe for providing infrastructure. Chat GPT (Open AI) was used to assist with language editing.

Financial support

This work was funded by the German Research Foundation (DFG grants SP673/27-1 and LI745/27-1). DC acknowledges support from Science Foundation Ireland through research grant 13/RC/2092_P2 (iCRAG Research Centre).

References

Barnes, C. J. and Schneider, D. A.: Late Cretaceous–Paleogene burial and exhumation history of the Southwestern Basement Province, Svalbard, revealed by zircon (U-Th)/He thermochronology, in: Circum-Arctic Structural Events: Tectonic Evolution of the Arctic Margins and Trans-Arctic Links with Adjacent Orogens, edited by: Piepjohn, K., Strauss, J. V., Reinhardt, L., and McClelland, W. C., Geological Society of America, 132–152, https://doi.org/10.1130/2018.2541(07), 2019.

Barnett-Moore, N., Müller, D. R., Williams, S., Skogseid, J., and Seton, M.: A reconstruction of the North Atlantic since the earliest Jurassic, Basin Res., 30, 160–185, https://doi.org/10.1111/bre.12214, 2018.

Batten, D. J.: Palynology of shales associated with the Kap Washington Group volcanics, central North Greenland, rapggu, 108, 15–23, https://doi.org/10.34194/rapggu.v108.7778, 1982.

Batten, D. J., Brown, P. E., Dawes, P. R., Higgins, A. K., Koch, B. E., Parsons, I., and Soper, N. J.: Peralkaline volcanicity on the Eurasia Basin margin, Nature, 294, 150–152, https://doi.org/10.1038/294150a0, 1981.

Beucher, R., Brown, R. W., Roper, S., Stuart, F., and Persano, C.: Natural age dispersion arising from the analysis of broken crystals: Part II. Practical application to apatite (U–Th)/He thermochronometry, Geochim. Cosmochim. Acta, 120, 395–416, https://doi.org/10.1016/j.gca.2013.05.042, 2013.

Birkelund, T. and Håkansson, E.: The Cretaceous of North Greenland—a stratigraphic and biogeographical analysis, Zitteliana, 7–25, 1983.

Blinova, M., Thorsen, R., Mjelde, R., and Inge Faleide, J.: Structure and evolution of the Bellsund Graben between Forlandsundet and Bellsund (Spitsbergen) based on marine seismic data., Norw. J. Geol., 89, 215–228, 2009.

Brotzer, A., Funck, T., Geissler, W. H., Piepjohn, K., Heyde, I., and Berglar, K.: Geophysical insights on the crustal structure of Greenland's northern continental margin towards the Morris Jesup Spur, Tectonophysics, 843, 229588, https://doi.org/10.1016/j.tecto.2022.229588, 2022.

Brown, P. E. and Parsons, I.: The Kap Washington Group volcanics, rapggu, 106, 65–68, https://doi.org/10.34194/rapggu.v106.7767, 1981.

https://doi.org/10.5194/egusphere-2026-1389
Preprint. Discussion started: 25 March 2026

Brown, P. E., Parsons, I., and Becker, S. M.: Peralkaline volcanicity in the Arctic Basin—the Kap Washington Volcanics, petrology and palaeotectonics, J. Geol. Soc., 144, 707–715, https://doi.org/10.1144/gsjgs.144.5.0707, 1987.

Brown, R. W., Beucher, R., Roper, S., Persano, C., Stuart, F., and Fitzgerald, P.: Natural age dispersion arising from the analysis of broken crystals. Part I: Theoretical basis and implications for the apatite (U–Th)/He thermochronometer, Geochim. Cosmochim. Acta, 122, 478–497, https://doi.org/10.1016/j.gca.2013.05.041, 2013.

Brune, S., Kolawole, F., Olive, J.-A., Stamps, D. S., Buck, W. R., Buiter, S. J. H., Furman, T., and Shillington, D. J.: Geodynamics of continental rift initiation and evolution, Nat Rev Earth Environ, 4, 235–253, https://doi.org/10.1038/s43017-023-00391-3, 2023.

Buchan, K. L. and Ernst, R. E.: Giant dyke swarms and the reconstruction of the Canadian Arctic islands, Greenland, Svalbard and Franz Josef Land, in: Dyke Swarms - Time Markers of Crustal Evolution, edited by: Hanski, E., Mertanen, S., Rämö, T., and Vuollo, J., Taylor & Francis Group, London, 27–48, https://doi.org/10.1201/NOE0415398992.ch2, 2006.

Buchan, K. L. and Ernst, R. E.: A giant circumferential dyke swarm associated with the High Arctic Large Igneous Province (HALIP), Gondwana Research, 58, 39–57, https://doi.org/10.1016/j.gr.2018.02.006, 2018.

Buggisch, W., Bachtadse, V., and Paech, H. J.: Paleomagnetic Investigations in Northeast Greenland and New Data from Devonian(?) and Late Carboniterous Rocks, Polarforschung, 69, 55–64, 2001.

Cherniak, D. J.: Diffusion in Accessory Minerals: Zircon, Titanite, Apatite, Monazite and Xenotime, Rev. Mineral. Geochem., 72, 827–869, https://doi.org/10.2138/rmg.2010.72.18, 2010.

Chew, D. M., Petrus, J. A., and Kamber, B. S.: U–Pb LA–ICPMS dating using accessory mineral standards with variable common Pb, Chem. Geol., 363, 185–199, https://doi.org/10.1016/j.chemgeo.2013.11.006, 2014.

Chung, W.-Y.: Earthquakes Along the Passive Margin of Greenland: Evidence for Postglacial Rebound Control, Pure and Applied Geophysics, 159, 2567–2584, https://doi.org/10.1007/s00024-002-8748-1, 2002.

Cochrane, R., Spikings, R. A., Chew, D., Wotzlaw, J.-F., Chiaradia, M., Tyrrell, S., Schaltegger, U., and Van Der Lelij, R.: High temperature (>350°C) thermochronology and mechanisms of Pb loss in apatite, Geochim. Cosmochim. Acta, 127, 39–56, https://doi.org/10.1016/j.gca.2013.11.028, 2014.

Crane, K., Doss, H., Vogt, P., Sundvor, E., Cherkashov, G., Poroshina, I., and Joseph, D.: The role of the Spitsbergen shear zone in determining morphology, segmentation and evolution of the Knipovich Ridge, Mar. Geophys. Res., 22, 153–205, 2001.

Croxton, C. A., Dawes, P. R., Soper, N. J., and Thomsen, E.: An occurrence of Tertiary shales from the Harder Fjord Fault, North Greenland fold belt, Peary Land, rapggu, 101, 61–64, https://doi.org/10.34194/rapggu.v101.7721, 1980.

Dam, G., Larsen, M., and Sønderholm, M.: Sedimentary response to mantle plumes: Implications from Paleocene onshore successions, West and East Greenland, Geology, 26, 207–210, https://doi.org/10.1130/0091-7613(1998)026%253C0207:SRTMPI%253E2.3.CO;2, 1998.

https://doi.org/10.5194/egusphere-2026-1389
Preprint. Discussion started: 25 March 2026

Damaske, D. and Estrada, S.: Correlation of aeromagnetic signatures and volcanic rocks over northern Greenland and the adjacent Lincoln Sea, in: ICAM IV Proceedings, 4th International Conference on Arctic Margins, Dartmouth, Nova Scotia, 224–232, 2003.

Dawes, P. R. and Peel, J. S.: The Northern Margin of Greenland from Baffin Bay to the Greenland Sea, in: The Arctic Ocean, edited by: Nairn, A. E. M., Churkin, M., and Stehli, F. G., Springer US, Boston, MA, 201–264, https://doi.org/10.1007/978-1-4757-1248-3_5, 1981.

Donelick, R. A.: Apatite etching characteristics versus chemical composition, Nuclear Tracks and Radiation Measurements, 21, 1359–0189, 1993.

Donelick, R. A., O'Sullivan, P. B., and Ketcham, R. A.: Apatite Fission-Track Analysis, Rev. Mineral. Geochem., 58, 49–94, https://doi.org/10.2138/rmg.2005.58.3, 2005.

Dörr, N., Lisker, F., Clift, P. D., Carter, A., Gee, D. G., Tebenkov, A. M., and Spiegel, C.: Late Mesozoic–Cenozoic exhumation history of northern Svalbard and its regional significance: Constraints from apatite fission track analysis, Tectonophysics, 514–517, 81–92, https://doi.org/10.1016/j.tecto.2011.10.007, 2012.

Dörr, N., Lisker, F., Piepjohn, K., and Spiegel, C.: Cenozoic development of northern Svalbard based on thermochronological data, Terra Nova, 31, 306–315, https://doi.org/10.1111/ter.12402, 2019a.

Dörr, N., Lisker, F., Jochmann, M., Rainer, T., Schlegel, A., Schubert, K., and Spiegel, C.: Subsidence, rapid inversion, and slow erosion of the Central Tertiary Basin of Svalbard: Evidence from the thermal evolution and basin modeling, in: Circum-Arctic Structural Events: Tectonic Evolution of the Arctic Margins and Trans-Arctic Links with Adjacent Orogens, edited by: Piepjohn, K., Strauss, J. V., Reinhardt, L., and McClelland, W. C., Geological Society of America, 169–188, https://doi.org/10.1130/2018.2541(09), 2019b.

Døssing, A., Stemmerik, L., Dahl-Jensen, T., and Schlindwein, V.: Segmentation of the eastern North Greenland oblique-shear margin — Regional plate tectonic implications, Earth Planet. Sci. Lett., 292, 239–253, https://doi.org/10.1016/j.epsl.2009.12.036, 2010.

Døssing, A., Hopper, J. R., Olesen, A. V., Rasmussen, T. M., and Halpenny, J.: New aero-gravity results from the Arctic: Linking the latest Cretaceous-early Cenozoic plate kinematics of the North Atlantic and Arctic Ocean, Geochem. Geophys. Geosyst., 14, 4044–4065, https://doi.org/10.1002/ggge.20253, 2013.

Døssing, A., Hansen, T. M., Olesen, A. V., Hopper, J. R., and Funck, T.: Gravity inversion predicts the nature of the Amundsen Basin and its continental borderlands near Greenland, Earth Planet. Sci. Lett., 408, 132–145, https://doi.org/10.1016/j.epsl.2014.10.011, 2014.

Døssing, A., Japsen, P., Watts, A. B., Nielsen, T., Jokat, W., Thybo, H., and Dahl-Jensen, T.: Miocene uplift of the NE Greenland margin linked to plate tectonics: Seismic evidence from the Greenland Fracture Zone, NE Atlantic, Tectonics, 35, 257–282, https://doi.org/10.1002/2015TC004079, 2016.

https://doi.org/10.5194/egusphere-2026-1389
Preprint. Discussion started: 25 March 2026

Dumais, M.-A., Gernigon, L., Olesen, O., Johansen, S. E., and Brönner, M.: New interpretation of the spreading evolution of the Knipovich Ridge derived from aeromagnetic data, Geophys. J. Int., 224, 1422–1428, https://doi.org/10.1093/gji/ggaa527, 2020.

Ehlers, B.-M. and Jokat, W.: Subsidence and crustal roughness of ultra-slow spreading ridges in the northern North Atlantic and the Arctic Ocean, Geophys. J. Int., 177, 451–462, https://doi.org/10.1111/j.1365-246X.2009.04078.x, 2009.

Eldrett, J. S., Harding, I. C., Wilson, P. A., Butler, E., and Roberts, A. P.: Continental ice in Greenland during the Eocene and Oligocene, Nature, 446, 176–179, https://doi.org/10.1038/nature05591, 2007.

Engen, Ø., Faleide, J. I., and Dyreng, T. K.: Opening of the Fram Strait gateway: A review of plate tectonic constraints, Tectonophysics, 450, 51–69, https://doi.org/10.1016/j.tecto.2008.01.002, 2008.

Estrada, S.: Basaltic Dykes in the Kap Washington and Frigg Fjord Areas (North Greenland), Polarforschung, 68, 19–23, 2000.

Estrada, S., Höhndorf, A., and Henjes-Kunst, F.: Cretaceous/Tertiary volcanism in North Greenland: the Kap Washington Group, Polarforschung, 69, 17–23, 2001.

Estrada, S., Tessensohn, F., and Sonntag, B.-L.: A Timanian island-arc fragment in North Greenland: The Midtkap igneous suite, Journal of Geodynamics, 118, 140–153, https://doi.org/10.1016/j.jog.2018.01.015, 2018.

Falcon-Lang, H. J., MacRae, R. A., and Csank, A. Z.: Palaeoecology of Late Cretaceous polar vegetation preserved in the Hansen Point Volcanics, NW Ellesmere Island, Canada, Palaeogeogr. Palaeoclimatol. Palaeoecol., 212, 45–64, https://doi.org/10.1016/j.palaeo.2004.05.016, 2004.

Farley, K. A.: Helium diffusion from apatite: General behavior as illustrated by Durango fluorapatite, J. Geophys. Res.: Solid Earth, 105, 2903–2914, https://doi.org/10.1029/1999JB900348, 2000.

Farley, K. A., Wolf, R. A., and Silver, L. T.: The effects of long alpha-stopping distances on (U-Th)/He ages, Geochim. Cosmochim. Acta, 60, 4223–4229, https://doi.org/10.1016/S0016-7037(96)00193-7, 1996.

Flowerdew, M. J., Fleming, E. J., Chew, D. M., Morton, A. C., Frei, D., Benedictus, A., Omma, J., Riley, T. R., Badenszki, E., and Whitehouse, M. J.: The Importance of Eurekan Mountains on Cenozoic Sediment Routing on the Western Barents Shelf, Geosciences, 13, 91, https://doi.org/10.3390/geosciences13030091, 2023.

Flowers, R. M., Ketcham, R. A., Shuster, D. L., and Farley, K. A.: Apatite (U–Th)/He thermochronometry using a radiation damage accumulation and annealing model, Geochim. Cosmochim. Acta, 73, 2347–2365, https://doi.org/10.1016/j.gca.2009.01.015, 2009.

Francis, J. E., Marenssi, S., Levy, R., Hambrey, M., Thorn, V. C., Mohr, B., Brinkhuis, H., Warnaar, J., Zachos, J., Bohaty, S., and DeConto, R.: Chapter 8 From Greenhouse to Icehouse – The Eocene/Oligocene in Antarctica, in: Developments in Earth and Environmental Sciences, vol. 8, Elsevier, 309–368, https://doi.org/10.1016/S1571-9197(08)00008-6, 2008.

Gaina, C., Gernigon, L., and Ball, P.: Palaeocene–Recent plate boundaries in the NE Atlantic and the formation of the Jan Mayen microcontinent, J. Geol. Soc., 166, 601–616, https://doi.org/10.1144/0016-76492008-112, 2009.

Gaina, C., Nikishin, A. M., and Petrov, E. I.: Ultraslow spreading, ridge relocation and compressional events in the East Arctic region: A link to the Eurekan orogeny?, Arktos, 1, 16, https://doi.org/10.1007/s41063-015-0006-8, 2015.

https://doi.org/10.5194/egusphere-2026-1389
Preprint. Discussion started: 25 March 2026

Gaina, C., Jakobsson, M., Straume, E. O., Timmermans, M.-L., Boggild, K., Bünz, S., Schlindwein, V., and Døssing, A.: Arctic Ocean bathymetry and its connections to tectonics, oceanography and climate, Nat. Rev. Earth Environ., 6, 211–227, https://doi.org/10.1038/s43017-025-00647-0, 2025.

Geissler, W. H., Estrada, S., Riefstahl, F., O'Connor, J. M., Spiegel, C., van den Boogard, P., and Klügel, A.: Middle Miocene magmatic activity in the Sophia Basin, Arctic Ocean—evidence from dredged basalt at the flanks of Mosby Seamount, Arktos, 5, 31–48, https://doi.org/10.1007/s41063-019-00066-8, 2019.

Gion, A. M., Williams, S. E., and Müller, R. D.: A reconstruction of the Eurekan Orogeny incorporating deformation constraints, Tectonics, 36, 304–320, https://doi.org/10.1002/2015TC004094, 2017.

Glebovsky, V. Yu., Kaminsky, V. D., Minakov, A. N., Merkur'ev, S. A., Childers, V. A., and Brozena, J. M.: Formation of the Eurasia Basin in the Arctic Ocean as inferred from geohistorical analysis of the anomalous magnetic field, Geotecton., 40, 263–281, https://doi.org/10.1134/S0016852106040029, 2006.

von Gosen, W. and Piepjohn, K.: Evolution of the Kap Cannon Thrust Zone (north Greenland), Tectonics, 18, 1004–1026, https://doi.org/10.1029/1999TC900035, 1999.

von Gosen, W. and Piepjohn, K.: Eurekan transpressive deformation in the Wandel Hav Mobile Belt (northeast Greenland), Tectonics, 22, 2001TC901040, https://doi.org/10.1029/2001TC901040, 2003.

Gregersen, S.: Earthquakes in Greenland, Bull. Geol. Soc. Den., 31, 11–27, 1982.

Guarnieri, P.: Pre-break-up palaeostress state along the East Greenland margin, J. Geol. Soc., 172, 727–739, https://doi.org/10.1144/jgs2015-053, 2015.

Guarnieri, P., Bojesen-Koefoed, J. A., Keulen, N., Konnerub-Madsen, J., Olivarius, M., Rasmussen, J. A., and Thomsen, T. B.: Strain partitioning during transpression in the Wandel Sea Basin (eastern North Greenland), 10th International Conference on Arctic Margins (ICAM-X), Bremen, Germany, abstract 35, https://doi.org/10.5281/zenodo.16810950, 2025a.

Guarnieri, P., Bojesen-Koefoed, J., Keulen, N., Konnerup-Madsen, J., Olivarius, M., Rasmussen, J. A., and Thomsen, T. B.: Tectonic evolution of the Wandel Sea Basin, Eastern North Greenland: Insights from structural data, detrital zircons geochronology, mineralogy, fluid inclusions, vitrinite reflectance and conodont color alteration index, in: SVALGEOBASE II: Tectono-thermal evolution of Svalbard - from metamorphic and magmatic processes to geothermal energy, Polish Academy of Sciences, 53–57, https://doi.org/10.25171/InstGeoph_PAS_Publs-2025-006, 2025b.

Haaland, L. C., Slagstad, T., Osmundsen, P. T., and Redfield, T.: U-Pb calcite ages date oblique rifting of the Arctic–North Atlantic gateway, Geology, 52, 615–619, https://doi.org/10.1130/G52140.1, 2024.

Håkansson, E.: Scaphitid ammonoids and inoceramid bivalves from Upper Cretaceous strata in North Greenland, in: Wandel Sea Basin: Basin Analysis, edited by: Håkansson, E., University of Copenhagen, Copenhagen; Denmark, Report 14, 1994.

Håkansson, E. and Pedersen, S. A. S.: Late Paleozoic to Tertiary tectonic evolution of the continental margin in North Greenland, in: Arctic geology and geophysics, vol. 8, edited by: Embry, A. E. and Balkwill, H. R., 331–348, 1982.

Håkansson, E. and Pedersen, S. A. S.: The Wandel Hav Strike-Slip Mobile Belt – A Mesozoic plate boundary in North Greenland, Bull. Geol. Soc. Den., 48, 149–158, https://doi.org/10.37570/bgsd-2001-48-08, 2001.

https://doi.org/10.5194/egusphere-2026-1389
Preprint. Discussion started: 25 March 2026

Håkansson, E. and Pedersen, S. A. S.: A healed strike-slip plate boundary in North Greenland indicated through associated pull-apart basins, Geol. Soc. Spec. Publ., 413, 143–169, https://doi.org/10.1144/SP413.10, 2015.

Håkansson, E. and Stemmerik, L.: Wandel Sea basin—A new synthesis of the late Paleozoic to Tertiary accumulation in North Greenland, Geology, 17, 683–686, https://doi.org/10.1130/0091-7613(1989)017%253C0683:WSBANS%253E2.3.CO;2, 1989.

Håkansson, E. and Stemmerik, L.: Wandel Sea Basin: basin analysis – a summary, rapggu, 165, 42–48, https://doi.org/10.34194/rapggu.v165.8276, 1995.

Håkansson, E., Heinberg, C., and Stemmerik, L.: The Wandel Sea Basin from Holm Land to Lockwood Ø, eastern North Greenland, rapggu, 106, 47–63, https://doi.org/10.34194/rapggu.v106.7766, 1981.

Håkansson, E., Heinberg, C., and Stemmerik, L.: Mesozoic and Cenozoic history of the Wandel Sea Basin area, North Greenland, bullggu, 160, 153–164, https://doi.org/10.34194/bullggu.v160.6716, 1991.

Håkansson, E., Piasecki, S., Konnerub-Madsen, J., Springer, N., and Thomse, E.: A late, thermal event in the Wandel Sea Basin; eastern North Greenland, in: Wandel Sea Basin: Basin Analysis, edited by: Håkansson, E., Copenhagen; Denmark, Report 13, 1994.

Hasebe, N., Barbarand, J., Jarvis, K., Carter, A., and Hurford, A. J.: Apatite fission-track chronometry using laser ablation ICP-MS, Chem. Geol., 207, 135–145, https://doi.org/10.1016/j.chemgeo.2004.01.007, 2004.

Higgins, A. K.: Geology of central and eastern North Greenland, rapggu, 128, 37–54, https://doi.org/10.34194/rapggu.v128.7923, 1986.

Higgins, A. K., Friderichsen, J. D., and Soper, N. J.: The North Greenland fold belt between central Johannes V Jensen Land and eastern Nansen Land, rapggu, 106, 35–45, https://doi.org/10.34194/rapggu.v106.7765, 1981.

Hovikoski, J., Pedersen, G. K., Alsen, P., Lauridsen, B. W., Svennevig, K., Nøhr-Hansen, H., Sheldon, E., Dybkjær, K., Bojesen-Koefoed, J. A., Piasecki, S., Bjerager, M., and Ineson, J. R.: The Jurassic–Cretaceous lithostratigraphy of Kilen, Kronprins Christian Land, eastern North Greenland, Bull. Geol. Soc. Den., 66, 61–112, https://doi.org/10.37570/bgsd-2018-66-04, 2018.

Jahren, A. H. and Sternberg, L. S. L.: Annual patterns within tree rings of the Arctic middle Eocene (ca. 45 Ma): Isotopic signatures of precipitation, relative humidity, and deciduousness, Geology, 36, 99–102, https://doi.org/10.1130/G23876A.1, 2008.

Japsen, P., Green, P. F., and Chalmers, J. A.: Thermo-tectonic development of the Wandel Sea Basin, North Greenland, GEUS Bulletin, 45, https://doi.org/10.34194/geusb.v45.5298, 2021.

Japsen, P., Green, P. F., and Chalmers, J. A.: Synchronous exhumation episodes across Arctic Canada, North Greenland and Svalbard in relation to the Eurekan Orogeny, Gondwana Research, 117, 207–229, https://doi.org/10.1016/j.gr.2023.01.011, 2023.

https://doi.org/10.5194/egusphere-2026-1389
Preprint. Discussion started: 25 March 2026

Jokat, W., Lehmann, P., Damaske, D., and Bradley Nelson, J.: Magnetic signature of North-East Greenland, the Morris Jesup Rise, the Yermak Plateau, the central Fram Strait: Constraints for the rift/drift history between Greenland and Svalbard since the Eocene, Tectonophysics, 691, 98–109, https://doi.org/10.1016/j.tecto.2015.12.002, 2016.

Ketcham, R. A.: Forward and Inverse Modeling of Low-Temperature Thermochronometry Data, Rev. Mineral. Geochem., 58, 275–314, https://doi.org/10.2138/rmg.2005.58.11, 2005.

Ketcham, R. A., Carter, A., Donelick, R. A., Barbarand, J., and Hurford, A. J.: Improved measurement of fission-track annealing in apatite using c-axis projection, Am. Mineral., 92, 789–798, https://doi.org/10.2138/am.2007.2280, 2007a.

Ketcham, R. A., Carter, A., Donelick, R. A., Barbarand, J., and Hurford, A. J.: Improved modeling of fission-track annealing in apatite, Am. Mineral., 92, 799–810, https://doi.org/10.2138/am.2007.2281, 2007b.

Ketcham, R. A., Gautheron, C., and Tassan-Got, L.: Accounting for long alpha-particle stopping distances in (U–Th–Sm)/He geochronology: Refinement of the baseline case, Geochim. Cosmochim. Acta, 75, 7779–7791, https://doi.org/10.1016/j.gca.2011.10.011, 2011.

Kokfelt, T. F., Willerslev, E., Bjerager, M., Heijboer, T., Keulen, N., Larsen, L. M., Pedersen, C. B., Pedersen, M., Svennevig, K., Sønderholm, M., Walentin, K. T., and Weng, W. L.: Seamless digital 1:500 000 scale geological map of Greenland, version 2.0, https://doi.org/10.22008/FK2/FWX5ET, 2023.

Kontak, D. J., Jensen, S. M., Dostal, J., Archibald, D. A., and Kyser, T. K.: Cretaceous Mafic Dyke Swarm, Peary Land, Northernmost Greenland: Geochronology And Petrology, The Canadian Mineralogist, 39, 997–1020, https://doi.org/10.2113/gscanmin.39.4.997, 2001.

Kristoffersen, Y. and Talwani, M.: Extinct triple junction south of Greenland and the Tertiary motion of Greenland relative to North America, Geol. Soc. Am. Bull., 88, 1037–1049, https://doi.org/10.1130/0016-7606(1977)88%253C1037:ETJSOG%253E2.0.CO;2, 1977.

Kristoffersen, Y., Hall, J. K., and Nilsen, E. H.: Morris Jesup Spur and Rise north of Greenland – exploring present seabed features, the history of sediment deposition, volcanism and tectonic deformation at a Late Cretaceous/early Cenozoic triple junction in the Arctic Ocean, Norw. J. Geol., 10, 1–53, https://doi.org/10.17850/njg101-1-4, 2021.

Läderach, C., Schlindwein, V., Schenke, H.-W., and Jokat, W.: Seismicity and active tectonic processes in the ultra-slow spreading Lena Trough, Arctic Ocean, Geophys J Int, 184, 1354–1370, https://doi.org/10.1111/j.1365-246X.2010.04926.x, 2011.

Langebroek, P. M., Nisancioglu, K. H., Lunt, D. J., Kathrine Pedersen, V., Nele Meckler, A., and Gasson, E.: On the possibility of ice on Greenland during the Eocene-Oligocene transition, EGU General Assembly, Vienna, Austria, EGU2017-3163, 2017.

Lundin, E. R. and Doré, A. G.: Non-Wilsonian break-up predisposed by transforms: examples from the North Atlantic and Arctic, Geol. Soc. Spec. Publ., 470, 375–392, https://doi.org/10.1144/SP470.6, 2019.

Lundin, E. R., Doré, A. G., Naliboff, J., and van Wijk, J.: Utilization of continental transforms in break-up: observations, models, and a potential link to magmatism, Geol. Soc. Spec. Publ., 524, 121–145, https://doi.org/10.1144/SP524-2021-119, 2023.

https://doi.org/10.5194/egusphere-2026-1389
Preprint. Discussion started: 25 March 2026

Lyberis, N. and Manby, G.: The Eurekan Deformation of North and Eastern North Greenland, Polarforschung, 69, 95–106, 2001.

Lyck, J. M. and Stemmerik, L.: Palynology and depositional history of the Paleocene? Thyra Ø Formation, Wandel Sea Basin, eastern North Greenland, ggub, 187, 21–49, https://doi.org/10.34194/ggub.v187.5193, 2000.

Manby, G.: Late Cretaceous-Early Tertiary dyke swarm of North Greenland its age, origins and tectonic significance, EGU General Assembly, Vienna, Austria, EGU2014-13687, 2014.

McKenzie, D. P. and Parker, R. L.: The North Pacific: an Example of Tectonics on a Sphere, Nature, 216, 1276–1280, https://doi.org/10.1038/2161276a0, 1967.

Meier, K., O'Sullivan, P., Jochmann, M. M., Wallrath, T., Monien, P., Piepjohn, K., Lisker, F., and Spiegel, C.: Shallow Thermal Anomalies and Their Role in the Breakup Evolution Along the Conjugate Margins of the Fram Strait (Svalbard and Eastern North Greenland), Indicated by Low-Temperature Thermochronology, Geochem. Geophys. Geosyst., 25, e2023GC011074, https://doi.org/10.1029/2023GC011074, 2024.

Meza-Cala, J. C., Minakov, A., Faleide, J. I., Abdelmalak, M. M., Shephard, G. E., Mattingsdal, R., Geissler, W. H., and Gaina, C.: Late Cenozoic intraplate volcanism as a trigger for hydrothermal venting in the Arctic southwestern Eurasia Basin, Commun. Earth Environ., 5, 654, https://doi.org/10.1038/s43247-024-01843-4, 2024.

Meza-Cala, J. C., Faleide, J. I., Minakov, A., Abdelmalak, M. M., Shephard, G. E., Geissler, W. H., Klitzke, P., Mattingsdal, R., and Gaina, C.: Crustal structure of the North Svalbard margin: Continental breakup and Eurasia Basin opening, Tectonophysics, 912, 230861, https://doi.org/10.1016/j.tecto.2025.230861, 2025.

Morgan, W. J.: Rises, trenches, great faults, and crustal blocks, J. Geophys. Res., 73, 1959–1982, https://doi.org/10.1029/JB073i006p01959, 1968.

Oakey, G. N. and Chalmers, J. A.: A new model for the Paleogene motion of Greenland relative to North America: Plate reconstructions of the Davis Strait and Nares Strait regions between Canada and Greenland, J. Geophys. Res.: Solid Earth, 117, B10401, https://doi.org/10.1029/2011JB008942, 2012.

O'Regan, M., Moran, K., Backman, J., Jakobsson, M., Sangiorgi, F., Brinkhuis, H., Pockalny, R., Skelton, A., Stickley, C., Koç, N., Brumsack, H., and Willard, D.: Mid-Cenozoic tectonic and paleoenvironmental setting of the central Arctic Ocean, Paleoceanography, 23, 2007PA001559, https://doi.org/10.1029/2007PA001559, 2008.

Paech, H.-J. and Estrada, S.: Coal rank data and tectonic structure of Mesozoic and Paleogene sediments in North Greenland, in: Circum-Arctic Structural Events: Tectonic Evolution of the Arctic Margins and Trans-Arctic Links with Adjacent Orogens, edited by: Piepjohn, K., Strauss, J. V., Reinhardt, L., and McClelland, W. C., Geological Society of America, 189–211, https://doi.org/10.1130/2018.2541(10), 2019.

de Paor, D. G., Bradley, D. C., Eisenstadt, G., and Phillips, S. M.: The Arctic Eurekan orogen: A most unusual fold-and-thrust belt, Geol. Soc. Am. Bull., 101, 952–967, https://doi.org/10.1130/0016-7606(1989)101%253C0952:TAEOAM%253E2.3.CO;2, 1989.

https://doi.org/10.5194/egusphere-2026-1389
Preprint. Discussion started: 25 March 2026

Paton, C., Hellstrom, J., Paul, B., Woodhead, J., and Hergt, J.: Iolite: Freeware for the visualisation and processing of mass spectrometric data, J. Anal. At. Spectrom., 26, 2508–2518, https://doi.org/10.1039/C1JA10172B, 2011.

Pedersen, G. K., Lauridsen, B. W., Svennevig, K., Bojesen-Koefoed, J. A., Nøhr-Hansen, H., and Alsen, P.: Burial history of a folded Cretaceous succession – A case study from the southern part of Kilen, eastern North Greenland, Cretaceous Res., 89, 22–35, https://doi.org/10.1016/j.cretres.2018.03.007, 2018.

Pedersen, S. A. S.: Regional geology and thrust fault tectonics in the southern part of the North Greenland fold belt, North Greenland, rapggu, 99, 79–87, https://doi.org/10.34194/rapggu.v99.7674, 1980.

Pedersen, S. A. S. and Håkansson, E.: Kronprins Christian Land Orogeny Deformational Styles of the End Cretaceous Transpressional Mobile Belt in Eastern North Greenland, Polarforschung, 69, 117–130, 2001.

Piasecki, S., Nøhr-Hansen, H., and Dalhoff, F.: Revised stratigraphy of Kap Rigsdagen beds, Wandel Sea Basin, North Greenland, nos, 51, 411–425, https://doi.org/10.1127/nos/2018/0444, 2018.

Piepjohn, K. and von Gosen, W.: Polyphase deformation at the Harder Fjord Fault Zone (North Greenland), Geol. Mag., 138, 407–434, https://doi.org/10.1017/S0016756801005660, 2001.

Piepjohn, K., von Gosen, W., Läufer, A., McClelland, W. C., and Estrada, S.: Ellesmerian and Eurekan fault tectonics at the northern margin of Ellesmere Island (Canadian High Arctic), zdgg, 164, 81–105, https://doi.org/10.1127/1860-1804/2013/0007, 2013.

Piepjohn, K., von Gosen, W., Tessensohn, F., Reinhardt, L., McClelland, W. C., Dallmann, W., Gaedicke, C., and Harrison, J. C.: Tectonic map of the Ellesmerian and Eurekan deformation belts on Svalbard, North Greenland, and the Queen Elizabeth Islands (Canadian Arctic), Arktos, 1, 12, https://doi.org/10.1007/s41063-015-0015-7, 2015.

Piepjohn, K., von Gosen, W., and Tessensohn, F.: The Eurekan deformation in the Arctic: an outline, J. Geol. Soc., 173, 1007–1024, https://doi.org/10.1144/jgs2016-081, 2016.

Piepjohn, K., Ruppel, A., Reinhardt, L., Blumenberg, M., Jochmann, M., and Spiegel, C.: Kinematics and age of deformation along the Trolle Land Fault System, Northeast Greenland, 10th International Conference on Arctic Margins (ICAM-X), Bremen, Germany, abstract 34, 2025.

Poirier, A. and Hillaire-Marcel, C.: Improved Os-isotope stratigraphy of the Arctic Ocean, Geophys. Res. Lett., 38, L14607, https://doi.org/10.1029/2011GL047953, 2011.

Raimondo, T., Hand, M., and Collins, W. J.: Compressional intracontinental orogens: Ancient and modern perspectives, Earth Sci. Rev., 130, 128–153, https://doi.org/10.1016/j.earscirev.2013.11.009, 2014.

Ritzmann, O. and Jokat, W.: Crustal structure of northwestern Svalbard and the adjacent Yermak Plateau: evidence for Oligocene detachment tectonics and non-volcanic breakup, Geophys. J. Int., 152, 139–159, https://doi.org/10.1046/j.1365-246X.2003.01836.x, 2003.

Roest, W. R. and Srivastava, S. P.: Sea-floor spreading in the Labrador Sea: A new reconstruction, Geology, 17, 1000–1003, https://doi.org/10.1130/0091-7613(1989)017%253C1000:SFSITL%253E2.3.CO;2, 1989.

https://doi.org/10.5194/egusphere-2026-1389
Preprint. Discussion started: 25 March 2026

Rosa, D., Majka, J., Thrane, K., and Guarnieri, P.: Evidence for Timanian-age basement rocks in North Greenland as documented through U-Pb zircon dating of igneous xenoliths from the Midtkap volcanic centers, Precambrian Res., 275, 394–405, https://doi.org/10.1016/j.precamres.2016.01.005, 2016.

Schouten, S., Eldrett, J., Greenwood, D. R., Harding, I., Baas, M., and Damsté, J. S. S.: Onset of long-term cooling of Greenland near the Eocene-Oligocene boundary as revealed by branched tetraether lipids, Geology, 36, 147–150, https://doi.org/10.1130/G24332A.1, 2008.

Shuster, D. L., Flowers, R. M., and Farley, K. A.: The influence of natural radiation damage on helium diffusion kinetics in apatite, Earth Planet. Sci. Lett., 249, 148–161, https://doi.org/10.1016/j.epsl.2006.07.028, 2006.

Smelror, M. and Larssen, G. B.: Are there Upper Cretaceous sedimentary rocks preserved on Sørkapp Land, Svalbard?, Norw. J. Geol., 96, 1–12, https://doi.org/10.17850/njg96-2-05, 2016.

Snow, J. E., Hellebrand, E., Von Der Handt, A., Nauret, F., Gao, Y., and Schenke, H. W.: Oblique nonvolcanic seafloor spreading in Lena Trough, Arctic Ocean, Geochem. Geophys. Geosyst., 12, Q10009, https://doi.org/10.1029/2011GC003768, 2011.

Soper, N. J. and Higgins, A. K.: A shallow detachment beneath the North Greenland fold belt: implications for sedimentation and tectonics, Geol. Mag., 124, 441–450, https://doi.org/10.1017/S0016756800017027, 1987.

Soper, N. J. and Higgins, A. K.: Late Cretaceous – Early Tertiary Deformation, North Greenland, in: Geology of the Innuitian Orogen and Arctic Platform of Canada and Greenland, edited by: Trettin, H. P., Geological Society of America, Geological Survey of Canada, 459–465, https://doi.org/10.1130/DNAG-GNA-E.459, 1991.

Soper, N. J., Dawes, P. R., and Higgins, A. K.: Cretaceous-Tertiary magmatic and tectonic events in North Greenland and the history of adjacent ocean basins, Meddr Grønland. Geosci., 8, 205–220, https://doi.org/10.7146/moggeosci.v8i.139582, 1982.

Spiegel, C., Kohn, B., Belton, D., Berner, Z., and Gleadow, A.: Apatite (U–Th–Sm)/He thermochronology of rapidly cooled samples: The effect of He implantation, Earth Planet. Sci. Lett., 285, 105–114, https://doi.org/10.1016/j.epsl.2009.05.045, 2009.

Spielhagen, R. F. and Tripati, A.: Evidence from Svalbard for near-freezing temperatures and climate oscillations in the Arctic during the Paleocene and Eocene, Palaeogeogr. Palaeoclimatol. Palaeoecol., 278, 48–56, https://doi.org/10.1016/j.palaeo.2009.04.012, 2009.

Srivastava, S. P.: Evolution of the Eurasian Basin and its implications to the motion of Greenland along Nares Strait, Tectonophysics, 114, 29–53, https://doi.org/10.1016/0040-1951(85)90006-X, 1985.

Stacey, J. S. and Kramers, J. D.: Approximation of terrestrial lead isotope evolution by a two-stage model, Earth Planet. Sci. Lett., 26, 207–221, https://doi.org/10.1016/0012-821X(75)90088-6, 1975.

Stemmerik, L., Larsen, B. D., and Dalhoff, F.: Tectono-stratigraphic history of northern Amdrup Land, eastern North Greenland: implications for the northernmost East Greenland shelf, ggub, 187, 7–19, https://doi.org/10.34194/ggub.v187.5192, 2000.

https://doi.org/10.5194/egusphere-2026-1389
Preprint. Discussion started: 25 March 2026

Stephenson, R. and Anudu, G.: The First-Order Crustal Structure and Basin Architecture of the Canadian Arctic Margin, Geochem. Geophys. Geosyst., 26, e2025GC012196, https://doi.org/10.1029/2025GC012196, 2025.

Stickley, C. E., St John, K., Koç, N., Jordan, R. W., Passchier, S., Pearce, R. B., and Kearns, L. E.: Evidence for middle Eocene Arctic sea ice from diatoms and ice-rafted debris, Nature, 460, 376–379, https://doi.org/10.1038/nature08163, 2009.

Stijl, F. W. van der and Mosher, G. Z.: The Citronen Fjord massive sulphide deposit, Peary Land, North Greenland: discovery, stratigraphy, mineralization and structural setting, ggub, 179, 1–44, https://doi.org/10.34194/ggub.v179.6270, 1998.

Straume, E. O., Nummelin, A., Gaina, C., and Nisancioglu, K. H.: Climate transition at the Eocene–Oligocene influenced by bathymetric changes to the Atlantic–Arctic oceanic gateways, Proc. Natl. Acad. Sci. U.S.A., 119, e2115346119, https://doi.org/10.1073/pnas.2115346119, 2022.

Svennevig, K., Guarnieri, P., and Stemmerik, L.: Tectonic inversion in the Wandel Sea Basin: A new structural model of Kilen (eastern North Greenland): Inversion in the Wandel Sea Basin, Tectonics, 35, 2896–2917, https://doi.org/10.1002/2016TC004152, 2016.

Svennevig, K., Guarnieri, P., and Stemmerik, L.: 3D restoration of a Cretaceous rift basin in Kilen, eastern North Greenland, Norw. J. Geol., 97, 21–32, https://doi.org/10.17850/njg97-1-02, 2017.

Svennevig, K., Alsen, P., and Guarnieri, P.: Descriptive text to the Geological map of Greenland, 1:100 000, Kilen 81 Ø.1 Syd, GEUS, Copenhagen, 29 pp., 2018.

Talwani, M. and Eldholm, O.: Evolution of the Norwegian-Greenland Sea, GSA Bulletin, 88, 969–999, https://doi.org/10.1130/0016-7606(1977)88%25253C969:EOTNS%25253E2.0.CO;2, 1977.

Tegner, C., Storey, M., Holm, P. M., Thorarinsson, S. B., Zhao, X., Lo, C.-H., and Knudsen, M. F.: Magmatism and Eurekan deformation in the High Arctic Large Igneous Province: 40Ar–39Ar age of Kap Washington Group volcanics, North Greenland, Earth Planet. Sci. Lett., 303, 203–214, https://doi.org/10.1016/j.epsl.2010.12.047, 2011.

Telmon, M., Betlem, P., Grundvåg, S. A., Kenji Horota, R., Minakov, A., Planke, S., Senger, K., Tegner, C., and Zastrozhnov, D.: The Seidfjellet Formation in NW Spitsbergen: A Window into Miocene Volcanism and Tectonics of Arctic-Atlantic Gateway, EGU General Assembly, Vienna, Austria, EGU25-3700, https://doi.org/10.5194/egusphere-egu25-3700, 2025.

Tessensohn, F. and Piepjohn, K.: Eocene compressive deformation in Arctic Canada, North Greenland and Svalbard and its plate tectonic causes, Polarforschung, 68, 121–124, 2000.

Thórarinsson, S. B., Holm, P. M., Tappe, S., Heaman, L. M., and Tegner, C.: Late Cretaceous–Palaeocene continental rifting in the High Arctic: U–Pb geochronology of the Kap Washington Group volcanic sequence, North Greenland, J. Geol. Soc., 168, 1093–1106, https://doi.org/10.1144/0016-76492011-018, 2011a.

Thórarinsson, S. B., Holm, P. M., Duprat, H., and Tegner, C.: Silicic magmatism associated with Late Cretaceous rifting in the Arctic Basin—petrogenesis of the Kap Kane sequence, the Kap Washington Group volcanics, North Greenland, Lithos, 125, 65–85, https://doi.org/10.1016/j.lithos.2011.01.013, 2011b.

https://doi.org/10.5194/egusphere-2026-1389
Preprint. Discussion started: 25 March 2026

Thórarinsson, S. B., Söderlund, U., Døssing, A., Holm, P. M., Ernst, R. E., and Tegner, C.: Rift magmatism on the Eurasia basin margin: U–Pb baddeleyite ages of alkaline dyke swarms in North Greenland, J. Geol. Soc., 172, 721–726, https://doi.org/10.1144/jgs2015-049, 2015.

Tripati, A. and Darby, D.: Evidence for ephemeral middle Eocene to early Oligocene Greenland glacial ice and pan-Arctic sea ice, Nat. Commun., 9, 1038, https://doi.org/10.1038/s41467-018-03180-5, 2018.

Tripati, A. K., Eagle, R. A., Morton, A., Dowdeswell, J. A., Atkinson, K. L., Bahé, Y., Dawber, C. F., Khadun, E., Shaw, R. M. H., Shorttle, O., and Thanabalasundaram, L.: Evidence for glaciation in the Northern Hemisphere back to 44 Ma from ice-rafted debris in the Greenland Sea, Earth Planet. Sci. Lett., 265, 112–122, https://doi.org/10.1016/j.epsl.2007.09.045, 2008.

Vamvaka, A., Pross, J., Monien, P., Piepjohn, K., Estrada, S., Lisker, F., and Spiegel, C.: Exhuming the Top End of North America: Episodic Evolution of the Eurekan Belt and Its Potential Relationships to North Atlantic Plate Tectonics and Arctic Climate Change, Tectonics, 38, 4207–4228, https://doi.org/10.1029/2019TC005621, 2019.

Vermeesch, P.: IsoplotR: A free and open toolbox for geochronology, Geoscience Frontiers, 9, 1479–1493, https://doi.org/10.1016/j.gsf.2018.04.001, 2018.

Wagner, G. A., Gleadow, A. J. W., and Fitzgerald, P. G.: The significance of the partial annealing zone in apatite fission-track analysis: Projected track length measurements and uplift chronology of the transantarctic mountains, Chemical Geology: Isotope Geoscience section, 79, 295–305, https://doi.org/10.1016/0168-9622(89)90035-3, 1989.

Winther, P. C., Troelsen, J., Holmen, K., Johnsen, P., Fristrup, B., and Knuth, E.: A Preliminary Account of the Danish Pearyland Expedition, 1948-9, ARCTIC, 3, 2–13, https://doi.org/10.14430/arctic3948, 1950.

Wolf, R. A., Farley, K. A., and Kass, D. M.: Modeling of the temperature sensitivity of the apatite (U–Th)/He thermochronometer, Chem. Geol., 148, 105–114, https://doi.org/10.1016/S0009-2541(98)00024-2, 1998.

Zinck-Jørgensen, K.: Structural development of the Herlufsholm Strand Basin, in: In: Wandel Sea Basin: Basin Analysis, vol. 19, University of Copenhagen, Copenhagen; Denmark, Report 19, 1994a.

Zinck-Jørgensen, K.: The Trolle Land Fault System, Kim Fjelde, eastern Peary Land, in: Wandel Sea Basin: Basin Analysis, University of Copenhagen, Copenhagen; Denmark, Report 18, 1994b.